NACA

C.1

RESEARCH MEMORANDUM

ALTITUDE-WIND-TUNNEL INVESTIGATION OF A 4000-POUND-

THRUST AXIAL-FLOW TURBOJET ENGINE

IV - ANALYSIS OF COMPRESSOR PERFORMANCE

By Robert O. Dietz, Jr. and Frank L. Suozzi

Flight Propulsion Research Laboratory
Cleveland, Ohio

NATIONAL ADVISORY COMMITTEE
FOR AERONAUTICS
WASHINGTON
August 5, 1948

RESTRICTED

NATIONAL ADVISORY COMMITTEE FOR AERONAUTICS

RESEARCH MEMORANDUM

ALTITUDE-WIND-TUNNEL INVESTIGATION OF A 4000-POUND-

THRUST AXIAL-FLOW TURBOJET ENGINE

IV - ANALYSIS OF COMPRESSOR PERFORMANCE

By Robert O. Dietz, Jr. and Frank L. Suozzi

SUMMARY

Operating characteristics of the 11-stage axial-flow compressor of a 4000-pound-thrust turbojet engine were determined from investigations of the complete engine in the Cleveland altitude wind tunnel. Two compressors were investigated: the standard compressor and one similar except that the blade angles of the rotor and stator blades were increased approximately 5° to obtain greater air flow. Three different turbine-nozzle areas were used to determine which combination of compressor and turbine nozzle gave optimum performance. The investigations covered a range of simulated altitudes from 5000 to 40,000 feet, ram pressure ratios from approximately 1.00 to 1.86, and compressor Mach numbers from 0.24 to 0.95. Compressor characteristics are presented as functions of air flow corrected to standard sea-level conditions and compressor Mach number.

Maximum adiabatic temperature-rise efficiency for both compressors was about 85 percent. The maximum efficiency was not obtained at design engine speed. At a corrected engine speed of 7600 rpm the following efficiencies, pressure ratios, and corrected air flows were observed:

Compressor	Turbine-nozzle area (sq.in.)	Efficiency (percent)	Compressor pressure ratio	Corrected air flow (lb/sec)	Approximate ram pressure ratio, P_1/p_0
Low flow	106.8	84	3.99	70.6	1.41-1.86
High flow	106.8	79	4.95	78.4	1.40-1.82
High flow	121	79	3.83	76.5	1.41

Variations of Reynolds number did not affect the efficiencies nor pressure ratios at a given compressor Mach number but decreasing Reynolds number decreased the corrected engine speed at which compressor stall occurred.

INTRODUCTION

A specific objective of the research program to investigate the 4000-pound-thrust axial-flow turbojet engine was the investigation of the compressor characteristics and the determination of how effectively the compressor is used in this engine. A summary of the over-all engine performance is given in references 1 and 2. The operational characteristics of the engine are discussed in reference 3.

An analysis of the performance characteristics of two compressors used in the turbojet engine is presented herein. The data were obtained from investigations of the complete engine. Characteristics of these compressors are of interest because they represent a modification of the free vortex design, which was made to obtain high efficiency and large capacity with a minimum over-all diameter.

The high-flow compressor unit reported does not represent any engine contemplated for production by the engine manufacturer, but does represent the initial attempt of the engine manufacturer to obtain increased performance by modifying the standard 4000-pound-thrust axial-flow unit with the quickest and simplest methods available at the time of the wind-tunnel research program.

The investigations were conducted in the Cleveland altitude wind tunnel with the engine operating at simulated flight conditions over a range of altitudes from 5000 to 40,000 feet, ram pressure ratios from approximately 1.00 to 1.86, and compressor Mach numbers from 0.24 to 0.95. Compressor Mach number is defined as the ratio of the tip speed of the compressor blades to the velocity of sound in air at the total temperature of the inlet air.

In an attempt to increase the thrust of the engine, the angle of the compressor rotor and stator blades was increased about 5° to obtain greater air flow. The modified or high-flow compressor was the same as the original or low-flow compressor except for the change in blade angle. Three sizes of turbine nozzle were also supplied for investigations made to determine which combination of compressor and turbine nozzle gives optimum performance.

SYMBOLS

The following symbols are used in the analysis:

A_t throat area of turbine nozzles, square feet

A_8 exhaust-nozzle area at tail rake, square feet

a local velocity of sound, feet per second

c_p specific heat at constant pressure, Btu per pound per ^{o}F

D rotor-blade tip diameter, feet

g ratio of absolute to gravitational units of mass, (32.174 lb/slug)

H_{ad} isentropic increase in total enthalpy per unit of mass for a given pressure ratio, foot-pounds per pound

J mechanical equivalent of heat, (778 ft-lb/Btu)

M compressor Mach number

N engine speed, rpm

n number of stages

P total pressure, pounds per square foot absolute

p static pressure, pounds per square foot absolute

P_1/p_0 ram pressure ratio

P_4/P_2 compressor pressure ratio

R gas constant, foot-pounds per pound per ^{o}F

T total temperature, ^{o}R

T_i indicated total temperature, ^{o}R

t static temperature, ^{o}R

U rotor tip speed, feet per second

W_a air flow, pounds per second

W_b bearing cooling air flow, pounds per second

W_f fuel flow, pounds per second

W_g gas flow, pounds per second

α thermocouple impact recovery factor, 0.85

γ ratio of specific heats, c_p/c_v

δ ratio of absolute total pressure at compressor inlet to
            absolute static pressure of NACA standard atmosphere at
            sea level

η adiabatic temperature-rise efficiency, percent

θ ratio of absolute total temperature at compressor inlet
            to absolute static temperature of NACA standard atmos-
            phere at sea level

ψ average pressure coefficient per stage, ratio of isen-
            tropic increase in energy of air across compressor to
            isentropic increase in energy it would have moving at
            rotor tip speed divided by number of compressor stages

$W_a\sqrt{\theta}/\delta$ air flow corrected to NACA standard atmospheric conditions
            at sea level, pounds per second

$N/\sqrt{\theta}$ engine speed corrected to NACA standard atmospheric condi-
            tions at sea level, rpm

Subscripts:

    The stations to which the subscripts refer are shown in figure 1.

o   free-stream conditions

1   cowling inlet

2   compressor inlet

3   compressor interstages

4   compressor outlet

5   turbine inlet

8   tail-pipe nozzle

DESCRIPTION OF COMPRESSOR

The 11-stage axial-flow compressor used for these investigations
has 5 principal components: inlet section, split stator casing,
outlet section, rotor, and blading (fig. 1). The assembled com-
pressor installed in the engine and the assembly with the lower half
of the compressor case removed are shown in figures 2 and 3, respec-
tively. The maximum outside diameter of the compressor, exclusive

of the inlet and outlet section, is $32\frac{1}{4}$ inches and the over-all

length is $43\frac{1}{4}$ inches.

Four streamlined struts in the inlet section support the front
rotor roller bearing. The wooden cowling (fig. 2) was attached for
static tests and a ram pipe (fig. 4) was attached directly to the
inlet section during ram determinations.

The stator casing, which has a constant inside diameter of
28.9 inches and is 28.75 inches long, is split, making the blading
accessible (fig. 3). Extraction holes are located at the fourth
and eighth compressor stages to furnish cooling air for the engine
bearings and turbine wheel, respectively, and to pressurize a
diaphragm that partly balances the axial thrust of the compressor.

The outlet section of the compressor serves as a diffuser and
also as a manifold for conducting air into the eight combustion
chambers. Support for the ball bearing on the outlet end of the
rotor is furnished by this diffuser section.

The rotor hub has a smooth conical surface for the first nine
stages and a cylindrical surface for the last two stages. The diam-
eter of the rotor hub at the compressor inlet is approximately
20 inches, increasing to 25 inches at the compressor outlet. Nominal
rotor-blade-tip clearance at assembly is approximately 0.046 inch.
The rotor-blade angle, measured from the plane of rotation, decreases
from the root to the tip with the rate of change decreasing toward
the blade tip. Rotor-blade thickness decreases from hub to tip.
Both rotor-blade and stator-blade lengths decrease from the first
stage to the eighth stage and are the same in the ninth, tenth, and
eleventh stages. Stator blades are fixed in the stator casing by
circumferential T slots as shown in figure 5. The stator blades
have no twist and are of constant thickness from the root to the tip.
Inlet and outlet guide vanes are also fixed in the stator casing by
circumferential T slots (fig. 5). These vanes have no twist nor taper
and have constant chord and thickness along the span.

The compressor blading is essentially of the free-vortex type with the first four stages modified to reduce the inlet Mach numbers at the blade-tip sections. In free-vortex designs, the tangential velocities relative to the blading must vary appreciably along the blade span. If the aerodynamic loading at the mean section is high, serious compressibility effects may be encountered at the compressor rotor-blade-tip sections in the first stages where the Mach number is highest. The blading design may be altered, as in the first four stages of the compressor investigated herein, to reduce the relative tangential velocities at the tip sections and thus minimize the compressibility effects.

The low-flow compressor was designed to deliver approximately 75 pounds of air per second at a pressure ratio of approximately 4.0 and an engine speed of 7600 rpm with standard sea-level conditions at the inlet. The high-flow compressor was designed to deliver approximately 12 percent more air at rated sea-level conditions.

INSTRUMENTATION

The low-flow and high-flow compressors were provided with the same instrumentation by the engine manufacturer and the NACA for recording static pressures, total pressures, and indicated temperatures. (See reference 1.) Stations at which surveys were taken are shown in figure 1. Drawings of the survey rakes and sectional views of measuring stations identifying and locating pressure tubes and thermocouples on the compressor are shown in figures 6 to 9. A wall orifice was installed in the compressor case between each row of stator blades to determine the static-pressure distribution.

The tail rake was instrumented as described in reference 1 to provide data for calculating gas flow through the engine.

ENGINE INSTALLATION

The engine was installed beneath a 7-foot-chord wing mounted in the 20-foot-diameter test section of the altitude wind tunnel. Flight conditions were simulated for various pressure altitudes by introducing dry refrigerated air from the tunnel make-up air system to the engine inlet through a closed duct connected to the compressor cowling. This air was throttled from sea-level pressure to the desired compressor-inlet pressure. A wooden cowling was used to introduce tunnel air into the engine for all static tests. Further information on runs and installation is given in reference 1.

PROCEDURE

Investigations were conducted over the full operable range of engine speeds for each condition. (See table I.) Changes in engine configuration other than turbine-nozzle area, exhaust-nozzle diameter, and compressor-blade angle are not included in table I because the changes in method of turbine fabrication, tail-pipe construction, and combustion-chamber design had negligible effect on compressor operating conditions.

METHODS OF CALCULATION

Compressor Mach number M is defined as the dimensionless ratio

$$M = U/a_2 = \frac{\pi DN}{60\sqrt{\gamma_2 g R T_2}}$$ (1)

Air flow through the compressor was calculated from pressures and temperatures measured at the tail rake, station 8. Gas flow through the exhaust nozzle was calculated from the following equation, derived in reference 1

$$W_g = \frac{p_8 A_8}{R}\sqrt{\frac{2Jgc_p}{t_8}\left[\left(\frac{P_8}{p_8}\right)^{\frac{\gamma_8-1}{\gamma_8}}-1\right]}$$

Air flow was then determined by subtracting the fuel flow W_f measured with a calibrated rotameter and adding the bearing cooling-air flow W_b

$$W_a = W_g - W_f + W_b$$

The bearing cooling-air flow varies from 0.25 to 0.75 percent of the total air flow. This variation is not large enough to significantly affect the compressor performance presented.

The corrected air flow is

$$\frac{W_a\sqrt{\theta}}{\delta}$$ (2)

Static temperatures were calculated from indicated-temperature readings by use of the equation

$$t = \frac{T_i}{1 + \alpha\left[(P/p)^{\frac{\gamma-1}{\gamma}}-1\right]}$$ (3)

Total temperature is then found from the adiabatic relation

$$T/t = (P/p)^{\frac{\gamma-1}{\gamma}} \qquad (4)$$

The following equation was used to calculate the adiabatic temperature-rise efficiency

$$\eta = \frac{(P_4/P_2)^{\frac{\gamma_3-1}{\gamma_3}} - 1}{T_4/T_2 - 1} \qquad (5)$$

where γ_3 is the ratio of the specific heats corresponding to the average static temperature of the air flowing through the compressor. Total temperatures used in equation (5) and the static temperatures used to obtain γ_3 were calculated from equations (3) and (4).

Average pressure coefficient per stage was defined by the following equation

$$\psi = \frac{H_{ad}}{n\frac{U^2}{2g}} = \frac{2}{n(\gamma_3 - 1)} \frac{(P_4/P_2)^{\frac{\gamma_3-1}{\gamma_3}} - 1}{M^2} \qquad (6)$$

RESULTS AND DISCUSSION

Method of Analysis

Compressor performance characteristics were determined only at conditions set by the over-all operating characteristics of the complete engine. These over-all characteristics determine an "operating line," which represents the relation of the pressure ratio across the compressor to the corrected air flow $\frac{W_a\sqrt{\theta}}{\delta}$ (equation (2)) when the engine speed is varied. The compressor operating line may also be represented as the relation between pressure ratio across the compressor and compressor Mach number. In the following discussion, both representations of the operating line are given.

The position of the operating line relative to the coordinates is primarily determined by the throat area of the turbine nozzles and the ratio of the gas temperature at the turbine inlet to the temperature of the air at the compressor inlet. When the pressure

ratio across the turbine nozzles is greater than critical (approximately 1.89), the relation between flow and compressor discharge pressure is approximately

$$W_a = \frac{kA_t P_5 \sqrt{\gamma_5}}{\sqrt{T_5}}$$

where k is an arbitrary constant. From this equation and the definitions of θ and δ, the corrected air flow $\frac{W_a \sqrt{\theta}}{\delta}$ is approximately given by

$$\frac{W_a \sqrt{\theta}}{\delta} = k_1 A_t \frac{P_5 \sqrt{\gamma_5}/P_2}{\sqrt{T_5/T_2}} \tag{7}$$

where k_1 is an arbitrary constant.

The compressor-outlet total pressure P_4 is equal to the turbine-inlet total pressure P_5 except for friction and momentum losses in the combustion chamber, which are small relative to the total pressure. Therefore, in equation (7), P_5/P_2 may be approximated by the compressor pressure ratio P_4/P_2 and the only operational variable that affects the relation of corrected air flow to compressor pressure ratio is the ratio of the gas temperature at the turbine inlet to the temperature of the air at the compressor inlet. When the pressure ratio across the turbine is less than critical, in addition to the foregoing factor, the back pressure in the turbine nozzle influences the relation of corrected air flow to compressor pressure ratio.

Position of Operating Line

Altitude effects. - The effect of altitude on the position of the operating line is negligible when either compressor is used (fig. 10). Turbine-nozzle areas for the two configurations presented in figure 10 were such that the same pressure ratio was obtained with both compressors at any given compressor Mach number.

Ram pressure effects. - The effects of ram on the position of the operating lines is shown in figure 11. The turbine-nozzle areas used in these investigations differed from the areas used for the investigations represented in figure 10; consequently, the pressure ratios across the compressors were different at any given compressor Mach number.

Increasing the ram pressure ratio above 1.4 for either compressor had no discernible effect on the compressor operating line. A shift of the line to the right, with respect to the coordinates, occurred for an increase in ram from 1.0 to 1.4. This effect is shown in figure 11(a), but is not so easily seen in figure 11(b).

Turbine-nozzle-area effects. - The effect of changing from large turbine nozzles to standard turbine nozzles is shown in figure 12. The 11-percent decrease of turbine-nozzle area reduced air flow by 10 percent at a pressure ratio of 3.5. This trend is consistent with the dependence of corrected air flow on turbine-nozzle area previously discussed.

Efficiency

Efficiencies of the low-flow and high-flow compressors are presented in figures 13 and 14, respectively. In each of these figures, the operating lines discussed in the preceding section have been replotted. Operating lines for static and ram tests are not shown together because the measured compressor characteristics were appreciably different for the two arrangements. These differences were apparently caused by turbulence and boundary layer in the engine inlet, which was caused by very high inlet velocity ratios existing at static conditions.

The maximum efficiency of the two compressors (figs. 13 and 14(b)) was about 85 percent   At a corrected engine speed of 7600 rpm, the following efficiencies were obtained:

Compressor	Turbine nozzle	Efficiency (percent)	Approximate ram pressure ratio, P_1/p_0
Low-flow	Standard	84	1.41-1.86
High-flow	Standard	79	1.40-1.82
High-flow	Large	79	1.41

The operating curves for the low-flow compressor at static test conditions with either the standard or small nozzles pass close to the region of maximum efficiency (fig. 13(a)). It is concluded that either condition of operation is satisfactory as far as compressor efficiency is concerned, but the use of smaller or larger nozzles would appreciably reduce the efficiency.

The efficiencies determined for the ram tests with the low-flow compressor (fig. 13(b)) are approximately equal to the efficiencies

found from static tests. The operating lines shown in figure 13(b) pass close to the region of maximum efficiency.

Static tests with the high-flow compressor combined with large turbine nozzles gave slightly lower efficiency than that obtained from the ram tests, as may be seen from figure 14. Higher efficiency was attained with the high-flow compressor when it was used with standard turbine nozzles (fig. 14(b)). The experimental data are insufficient to show whether the high-flow compressor combined with standard turbine nozzles is optimum where compressor efficiency is concerned but the operation line for the combination is judged to pass close to the region of maximum efficiency. Use of the larger turbine nozzles definitely reduces compressor efficiency.

In figures 15 to 17, $(T_4/T_2) - 1$ is plotted against $(P_4/P_2)^{\frac{\gamma-1}{\gamma}} - 1$. Values taken from these curves were used in equation (5) to calculate compressor efficiency. This method of treating the data gave more consistent values of efficiency than the method in which efficiencies were calculated directly from the data. Efficiency curves constructed from figures 15 to 17 are shown in figures 18 and 19.

Because compressor efficiency is equal to the abscissa divided by the ordinate of the curves in figures 15 to 17, it is concluded from figure 15 that the effect of altitude (Reynolds number) variation on efficiency is negligible because points representing data obtained at all altitudes with one compressor fall on a single line.

Pressures

Pressure ratios. - The relations among pressure ratio, corrected air flow, and Mach number were shown in figures 10 to 12. Pressure ratios for the low-flow and high-flow compressors at the corrected engine speed of 7600 rpm are listed in the following table:

Compressor	Turbine nozzle	Compressor pressure ratio	Approximate ram pressure ratio, P_1/p_0
Low flow	Standard	3.99	1 41-1.86
High flow	Standard	4.95	1.40-1.82
High flow	Large	3.83	1.41

Changes in altitude cause variations of Reynolds number and the effect of this variation on the relation among pressure ratio, Mach number, and corrected air flow is negligible (fig. 10).

The same conclusion was found to be applicable to the static pres-
sures at the individual stages of both compressors. Figure 20 shows
the stage-to-stage variation of static pressures for low-flow and
high-flow compressors.

Pressure coefficients. - The average pressure coefficient ψ
for each stage of the compressor is plotted in figures 21 and 22,
which are similar to figures 13 and 14 except that pressure coeffi-
cients are shown instead of efficiencies. Pressure coefficients
were found from figures 23 to 25 in which the relation between
pressure coefficient and corrected air flow is presented. These
coefficients were calculated from equation (6).

Pressure coefficients determined at a corrected engine speed
of 7600 rpm are listed in the following table:

Compressor	Turbine nozzle	Compressor pressure coefficient	Approximate ram pressure ratio, P_1/p_0
Low flow	Standard	0.300	1.41-1.86
High flow	Standard	.346	1.40-1.82
High flow	Large	.292	1.41

Figures 21 and 22 show that the operating line always falls to the
right of the region in which a maximum pressure coefficient may be
obtained. The high-flow compressor gave somewhat higher pressure
coefficients than the low-flow compressor, the maximum values
being 0.378 and 0.333, respectively.

Velocity Profile at Compressor Outlet

Outlet velocity profiles were plotted in figures 26 and 27
for the low-flow and high-flow compressors at various altitudes and
engine speeds. At various pressure altitudes and low engine speeds,
the velocity distribution across the diffuser remained approximately
constant for both compressors but at high speeds it varied consider-
ably.

Compressor Stall

Compressor stall limited the maximum engine speed when the
combination of high-flow compressor and small turbine nozzles was
used. Figure 28 shows that the corrected engine speed at which
stall occurs decreases with increasing altitude. This variation
indicates that changes of Reynolds number probably have an appre-
ciable effect on compressor stall; decreasing Reynolds number
decreases the corrected engine speed at which stall occurs.

SUMMARY OF RESULTS

For the range of compressor operation obtainable in the investigation of a 4000-pound-thrust axial-flow turbojet engine in the altitude wind tunnel the following performance results for the compressors were found:

1. Maximum adiabatic temperature-rise efficiency for both the low-flow and high-flow compressors was about 85 percent. The maximum efficiency was not obtained at design engine speed. At a corrected engine speed of 7600 rpm, the following efficiencies and corrected air flows were obtained:

Compressor	Turbine nozzle	Efficiency (percent)	Corrected air flow (lb/sec)	Approximate ram pressure ratio, P_1/p_0
Low flow	Standard	84	70 6	1.41-1.86
High flow	Standard	79	78.4	1.40-1.82
High flow	Large	79	76.5	1.41

2. The operating curves for the engine with the following combinations of compressors and turbine nozzles were near optimum where compressor efficiency was concerned:

Low-flow compressor; small turbine nozzles
Low-flow compressor; standard turbine nozzles
High-flow compressor; standard turbine nozzles

The combination of high-flow compressor and large turbine nozzles gave efficiencies that were appreciably lower than the other three combinations.

3. Altitude had no measurable influence on the relation of efficiency to corrected air flow and compressor Mach number. This result is interpreted to mean that the effect of the Reynolds number was negligible

4. Compressor pressure ratios obtained at the corrected engine speed of 7600 rpm are:

Compressor	Turbine nozzle	Compressor pressure ratio	Approximate ram pressure ratio, P_1/p_0
Low flow	Standard	3.99	1.41-1.86
High flow	Standard	4.95	1.40-1.82
High flow	Large	3.83	1.41

5. The high-flow compressor gave somewhat higher pressure coefficients than the low-flow compressor; the maximum values were 0.378 and 0.333, respectively.

6. Compressor stall limited the maximum operating speed of the engine when the high-flow compressor was used in combination with small turbine nozzles. The corrected engine speed at which stall occurred decreased with increasing altitude.

Flight Propulsion Research Laboratory,
    National Advisory Committee for Aeronautics,
        Cleveland, Ohio.

REFERENCES

1. Fleming, William A.: Altitude-Wing-Tunnel Investigation of a 4000-Pound-Thrust Axial-Flow Turbojet Engine. I - Performance and Windmilling Drag Characteristics. NACA RM No. E8F09, 1948.

2. Fleming, William A., and Golladay, Richard L.: Altitude-Wind-Tunnel Investigation of a 4000-Pound-Thrust Axial-Flow Turbojet Engine. III - Performance Characteristics with the High-Flow Compressor. NACA RM No. E8F09b, 1948.

3. Fleming, William A.: Altitude-Wind-Tunnel Investigation of a 4000-Pound-Thrust Axial-Flow Turbojet Engine. II - Operational Characteristics. NACA RM No. E8F09a, 1948.

TABLE I - COMPRESSOR CONFIGURATIONS USED IN INVESTIGATION

OF 4000-POUND-THRUST AXIAL-FLOW TURBOJET ENGINE

Configu- ration (a)	Type of com- pressor	Turbine-nozzle area (sq.in.)	Exhaust- nozzle diameter (in.)	Simulated altitude (ft)	Ram pres- sure ratio
1	Low flow	101.9 (small)	$16\frac{1}{4}$	5,000 10,000 20,000 30,000	1.00 1.00 1.02 1.00
3	Low flow	106.8 (standard)	$16\frac{3}{4}$	10,000 40,000	1.21 1.20 1.62
4	Low flow	106.8	$16\frac{3}{4}$	40,000	1.41 1.86
5	Low flow	106.8	$16\frac{3}{4}$	40,000	1.02
6	High flow	106.8	18	20,000 40,000	1.38 1.40 1.82
11	High flow	121 (large)	18	5,000 20,000 30,000	1.01 1.02 1.01
12	High flow	121	$19\frac{1}{2}$	40,000	1.41

aConfigurations are designated and discussed in reference 3.
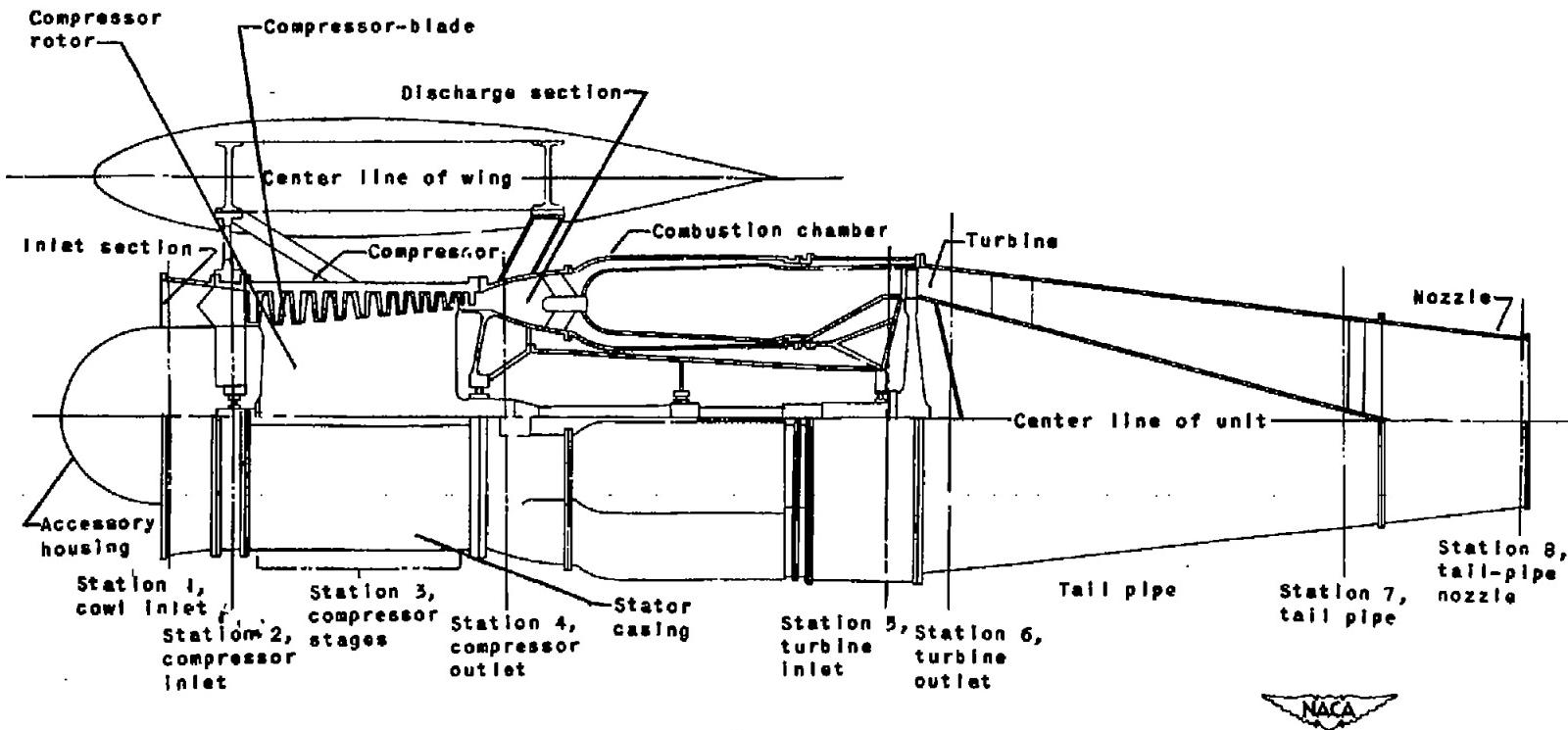
Figure I. — Side view of axial-flow turbojet-engine installation showing measuring stations.
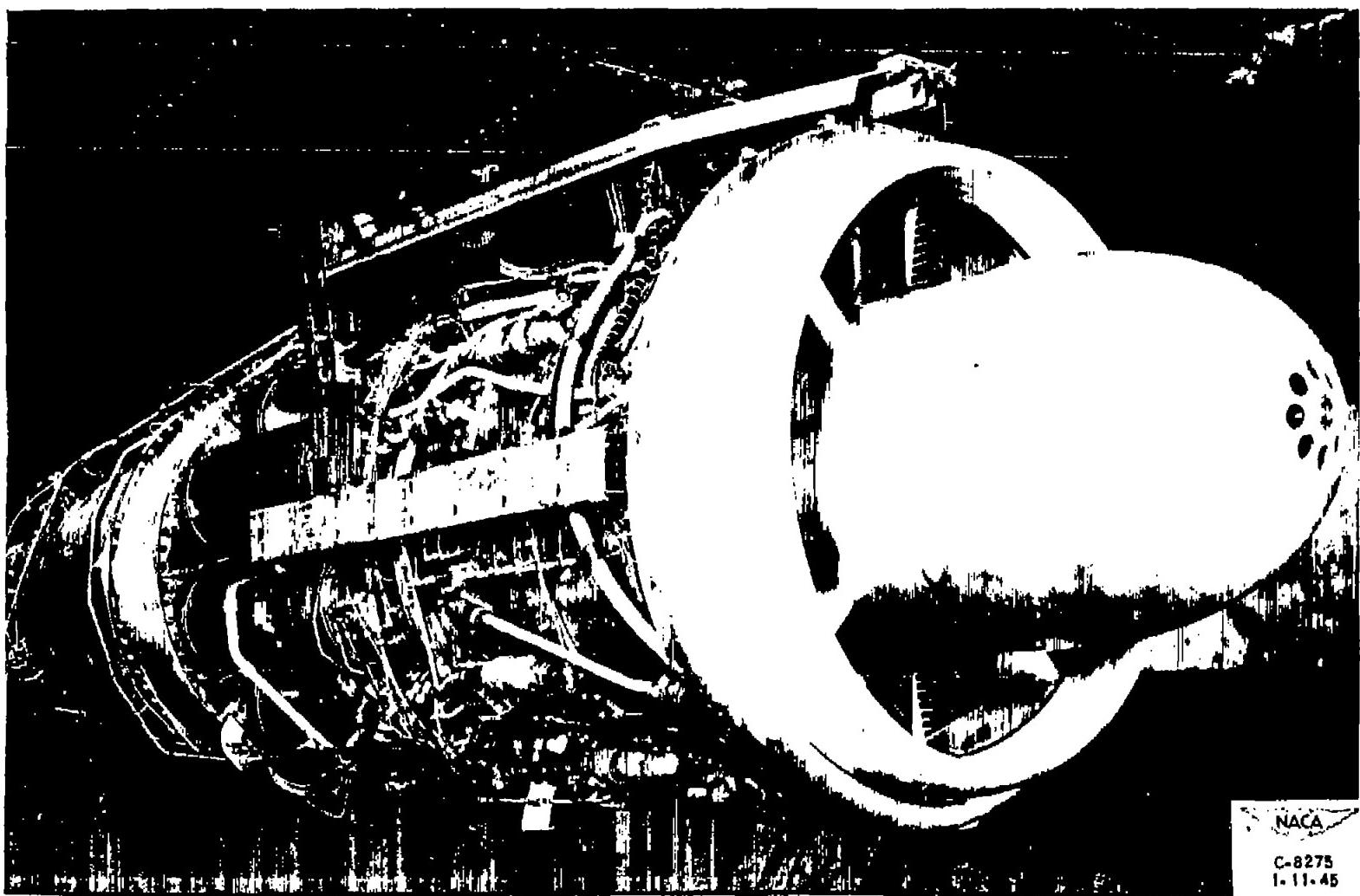
Figure 2. — Axial-flow turbojet engine in Cleveland altitude wind tunnel with streamlined fairing removed from compressor case.
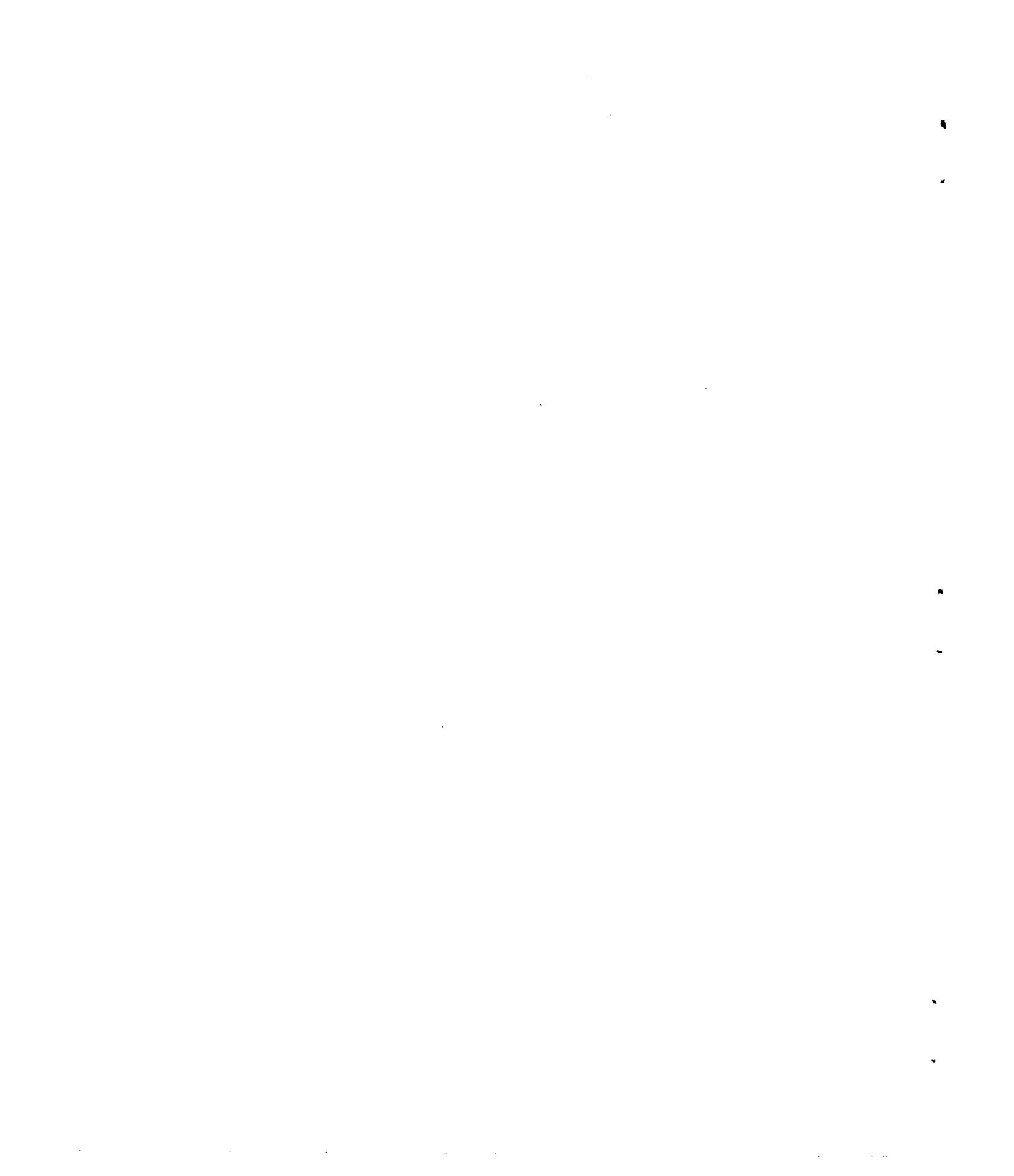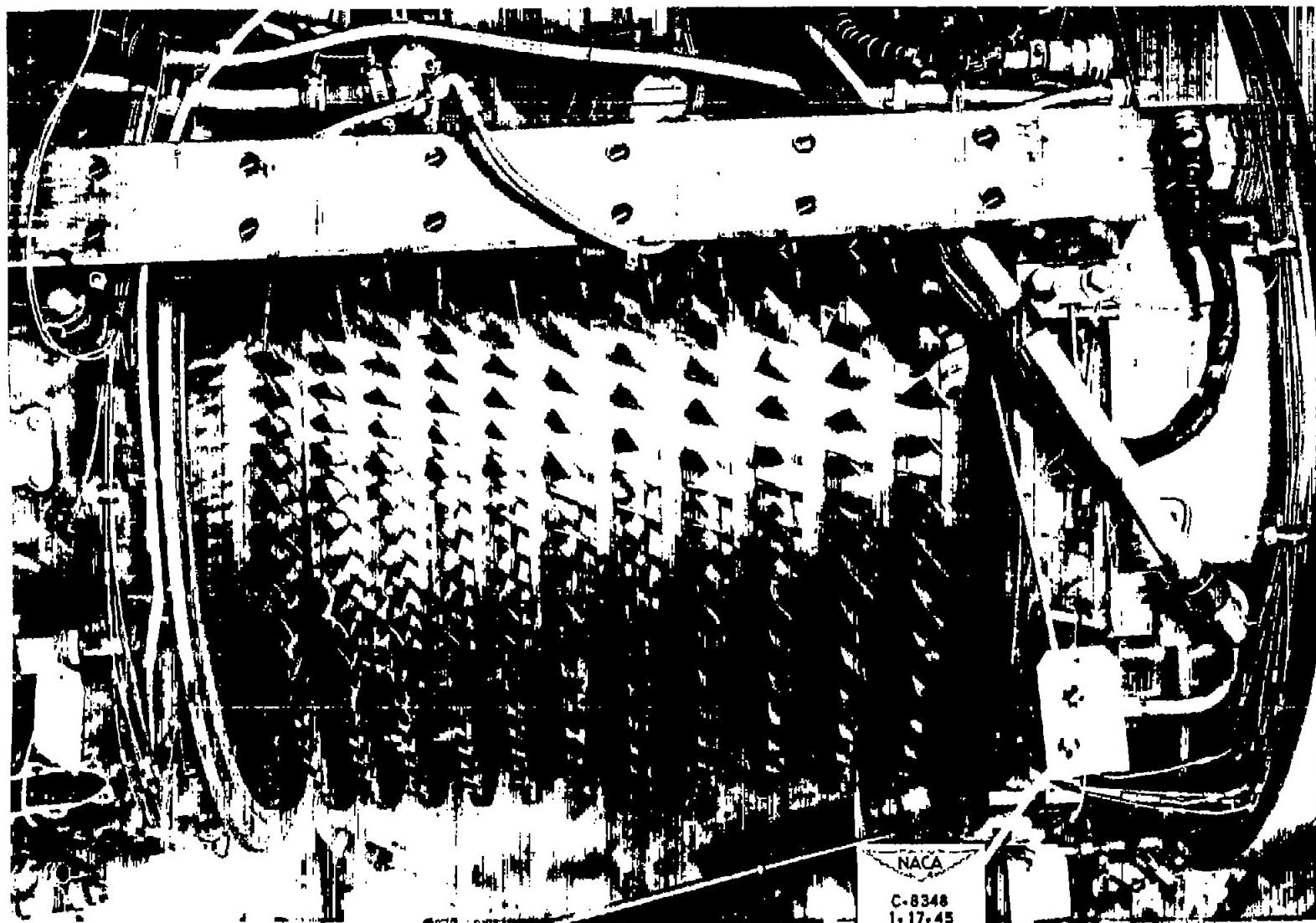
Figure 3. — Axial-flow turbojet engine with lower half of compressor casing removed.

Orifice flange
static-pressure
taps

12-7½"

28'-1¾"

9'-5¾"

12'-0"

6"

2'-0¼"

29¾ I.D.

Engine

Movable pipe

Orifice plate

20"

Upstream thermocouples

Upstream static-pressure taps

Slip Joint

Stationary pipe
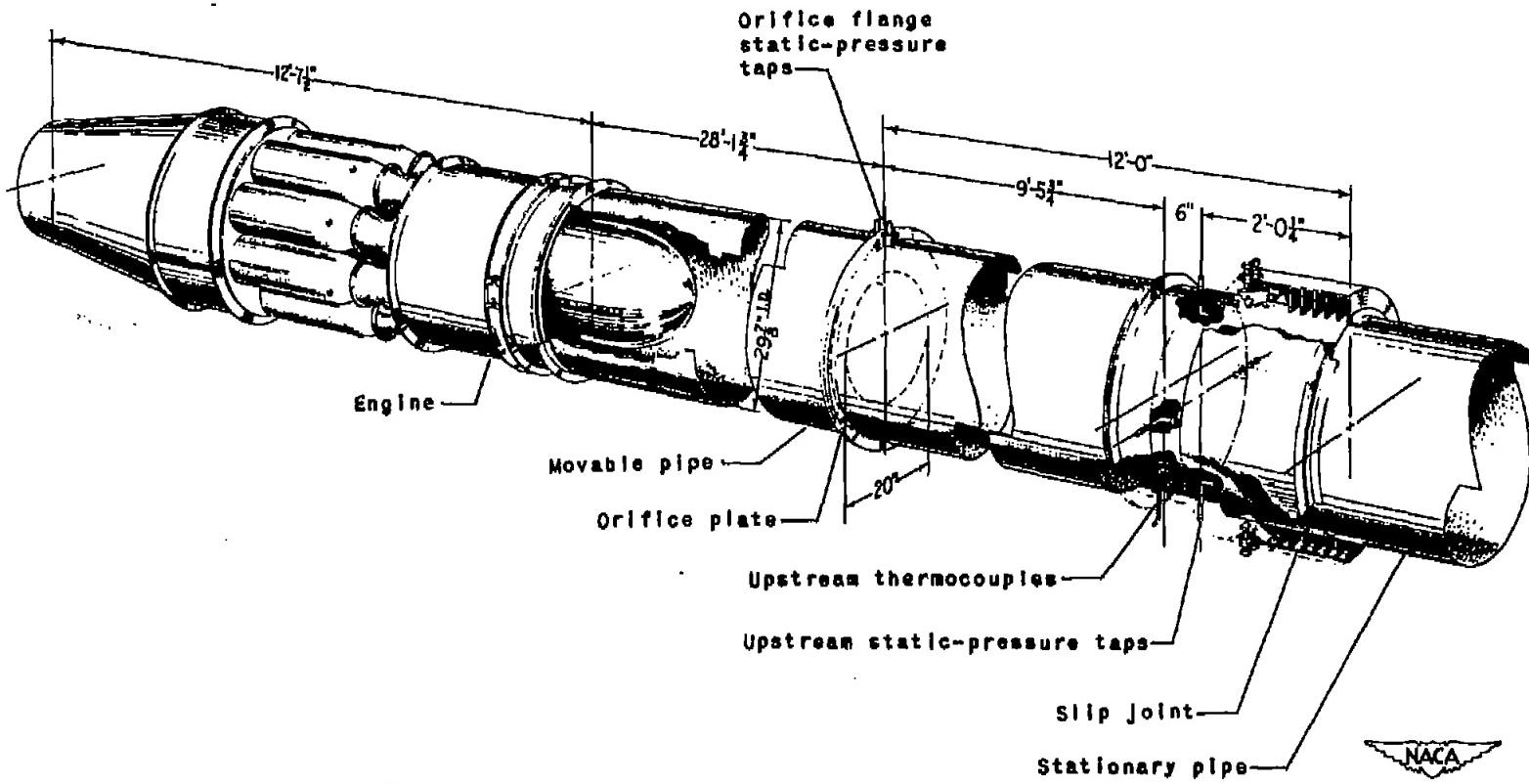
NACA

Figure 4. — Installation of ram pipe from tunnel make-up air pipe to engine inlet for supplying air
at ram pressures.
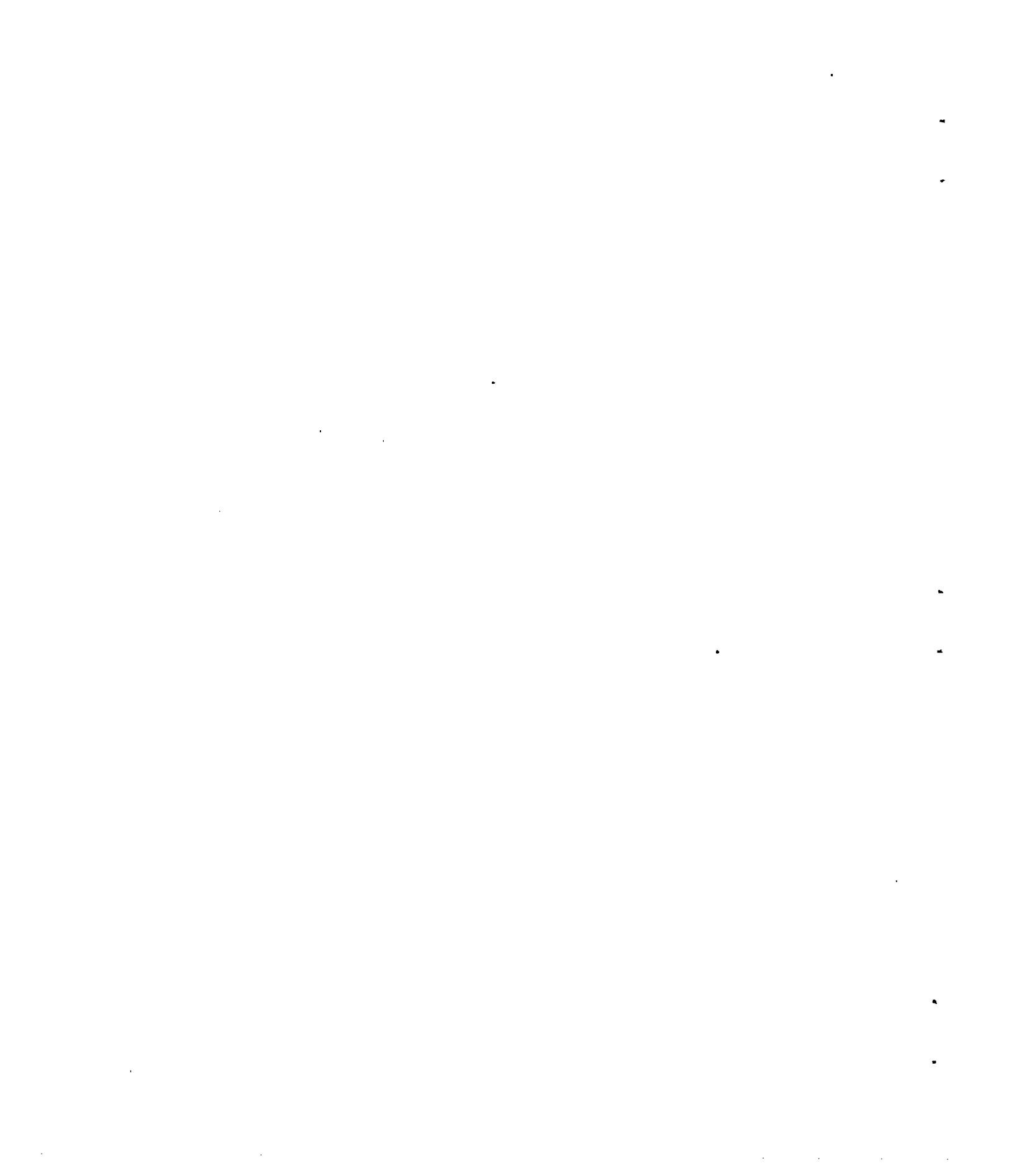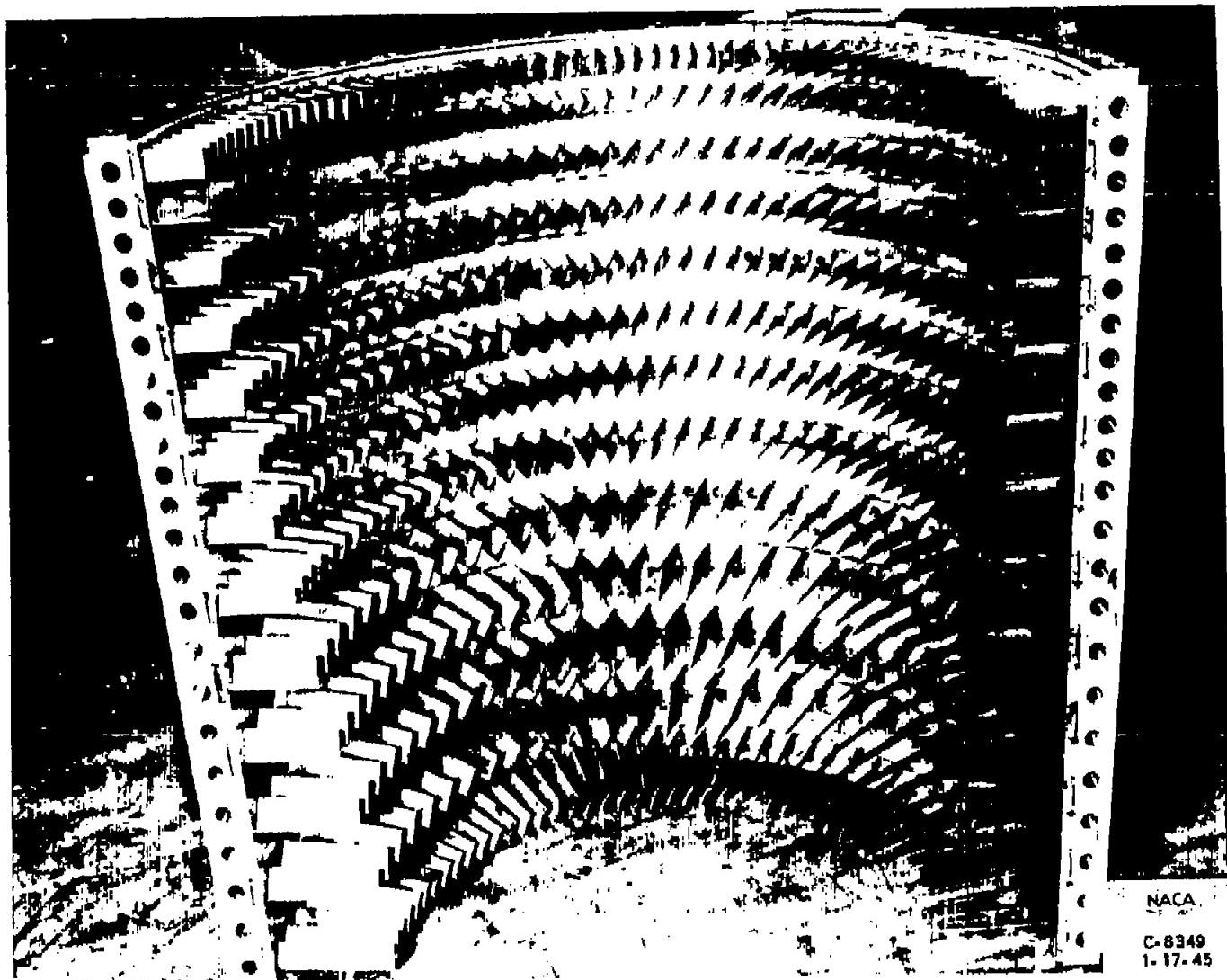
Figure 5. — Interior of axial-flow turbojet engine compressor housing showing stator blades, inlet guide vanes, and one row of straightening vanes after eleventh stage.
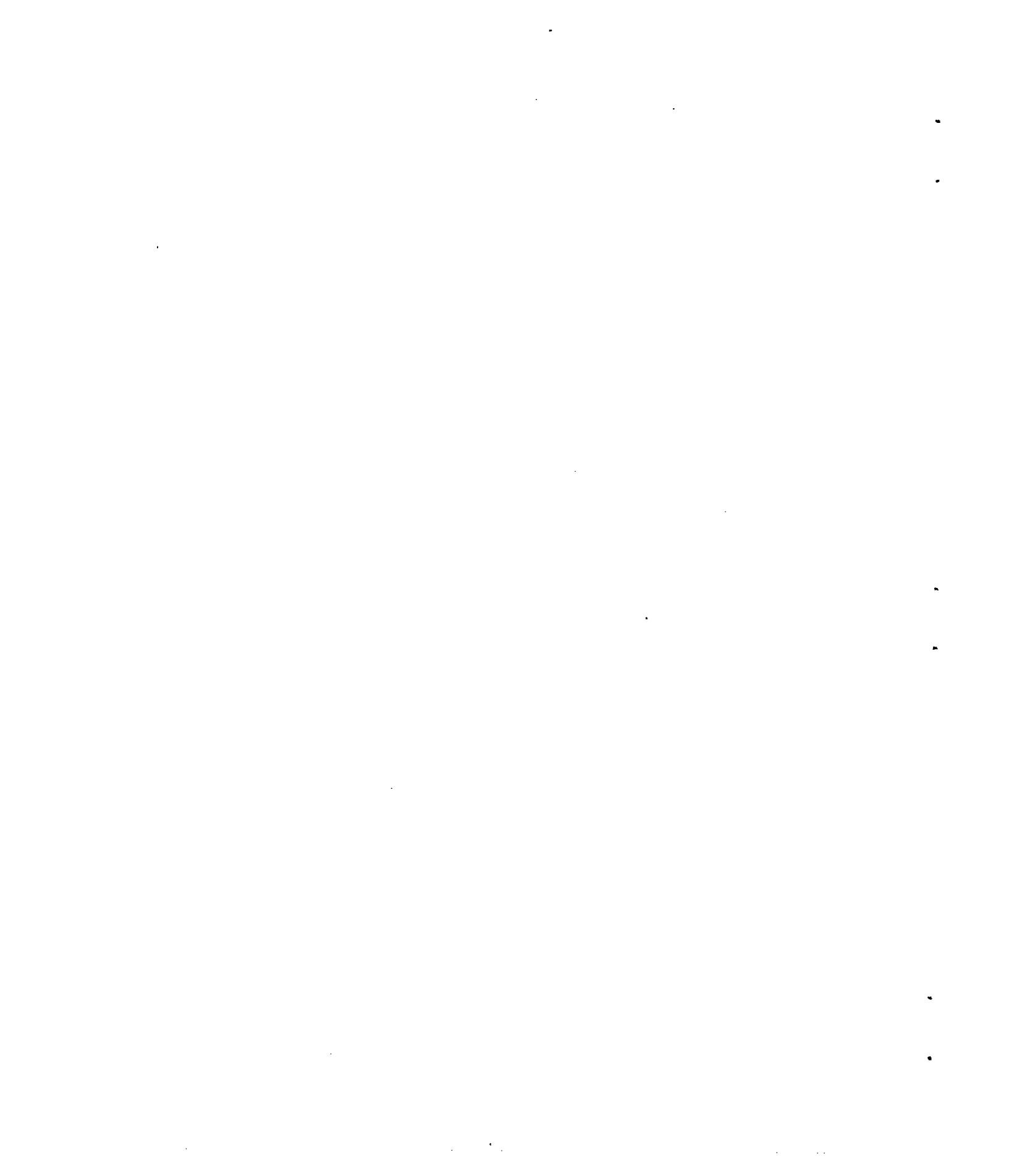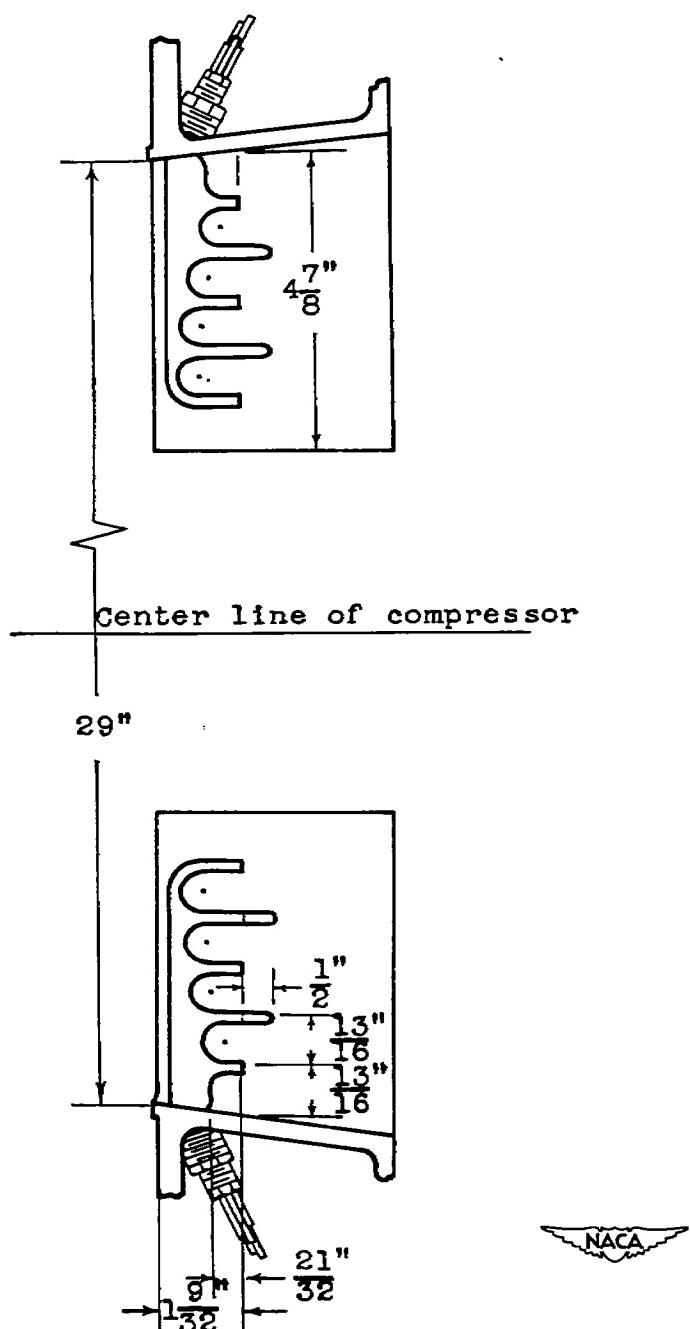
Figure 6.— Details of total— and static—pressure—tube
installation at compressor inlet, station 2, $1\frac{9}{32}$
inches ahead of front flange of compressor housing.
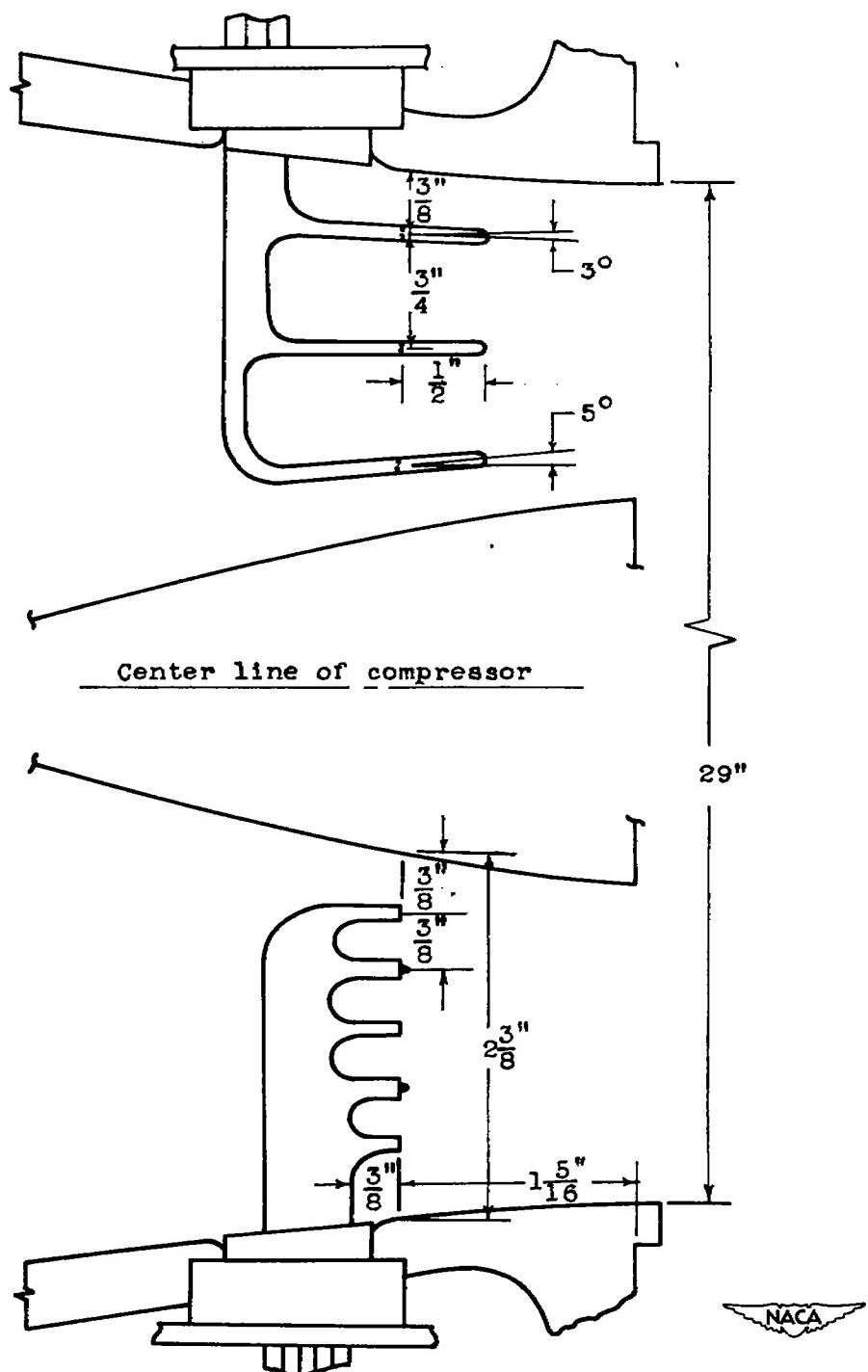
Figure 7.- Details of total-pressure-tube and thermocouple
    installation at compressor outlet, station 4, $1\frac{5}{16}$ inches
    behind rear flange of compressor housing.

582
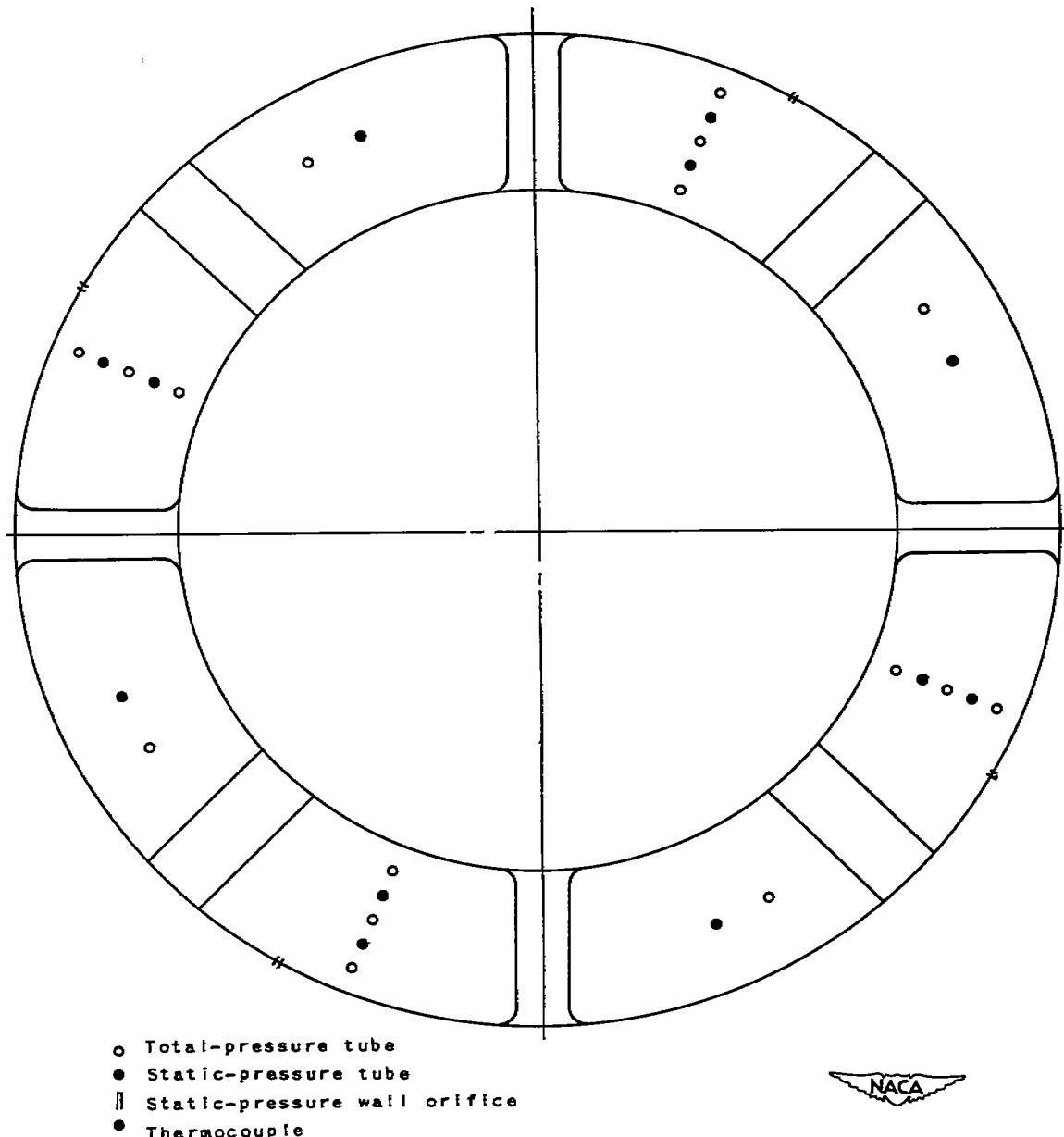
Figure 8. - Location of survey instrumentation at compressor inlet, station 2, $1\frac{9}{32}$ inches ahead of front flange of compressor housing.

o Total-pressure tube
● Static-pressure tube
‖ Static-pressure wall orifice
● Thermocouple
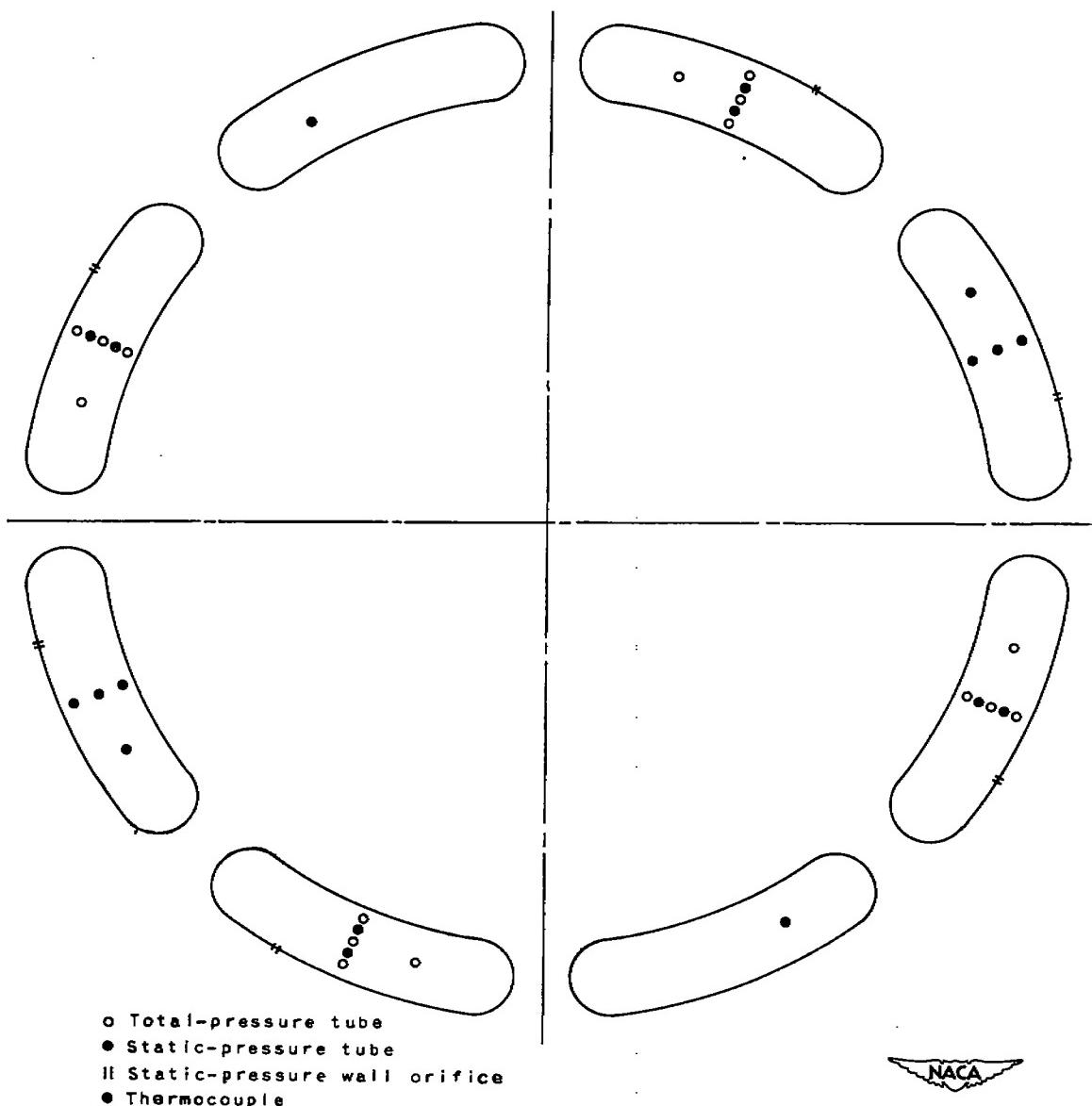
Figure 9. - Location of survey instrumentation at compressor outlet, station 4, $1\frac{5}{16}$ inches behind rear flange of compressor housing.

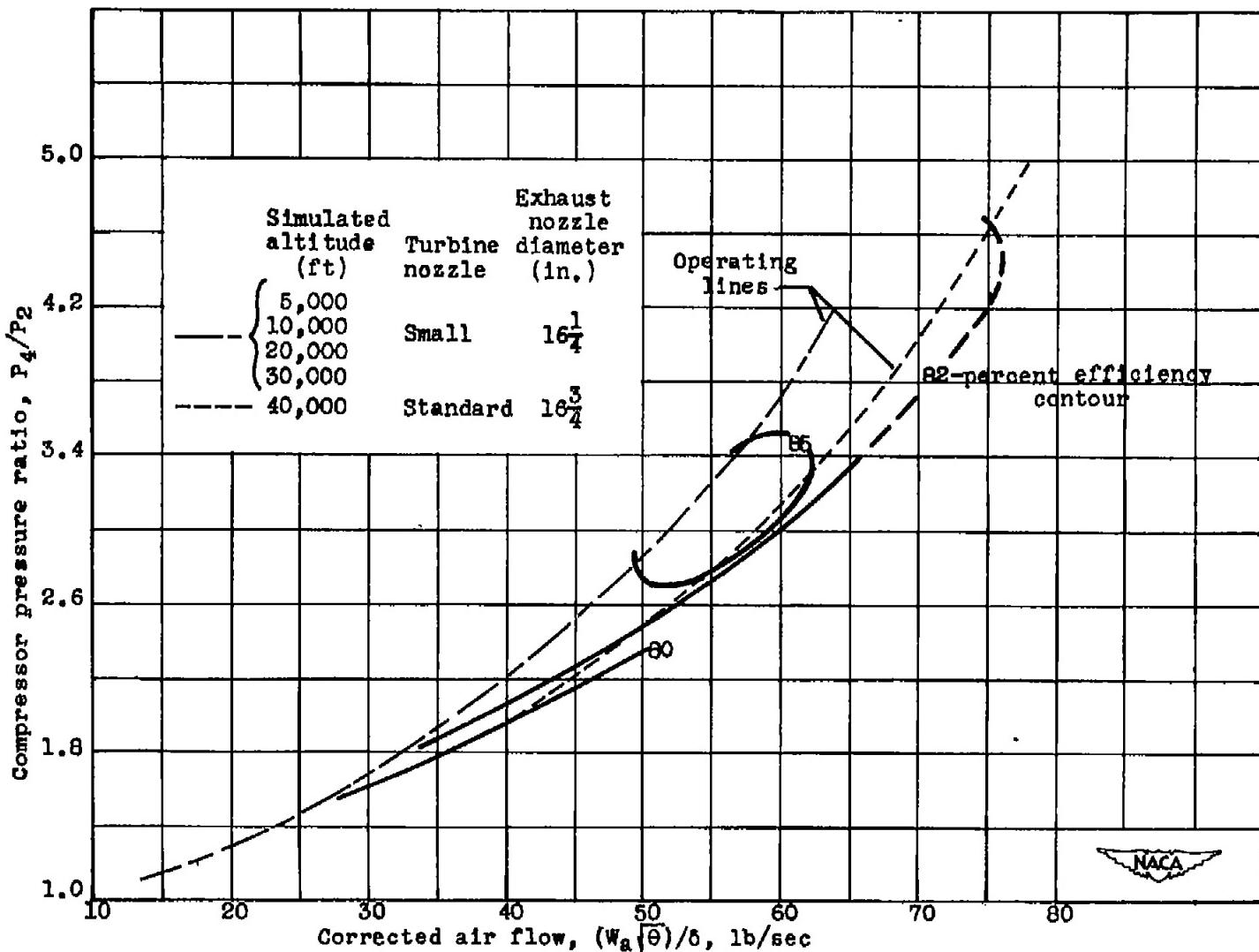| Simulated altitude (ft)	Compressor	Turbine nozzle	Exhaust nozzle diameter (in.)
O 5,000	Low-flow	Small	$16\frac{1}{4}$
□ 10,000	Low-flow	Small	$16\frac{1}{4}$
◇ 20,000	Low-flow	Small	$16\frac{1}{4}$
△ 30,000	Low-flow	Small	$16\frac{1}{4}$
Q 5,000	High-flow	Large	18
◈ 20,000	High-flow	Large	18
⬗ 30,000	High-flow	Large	18
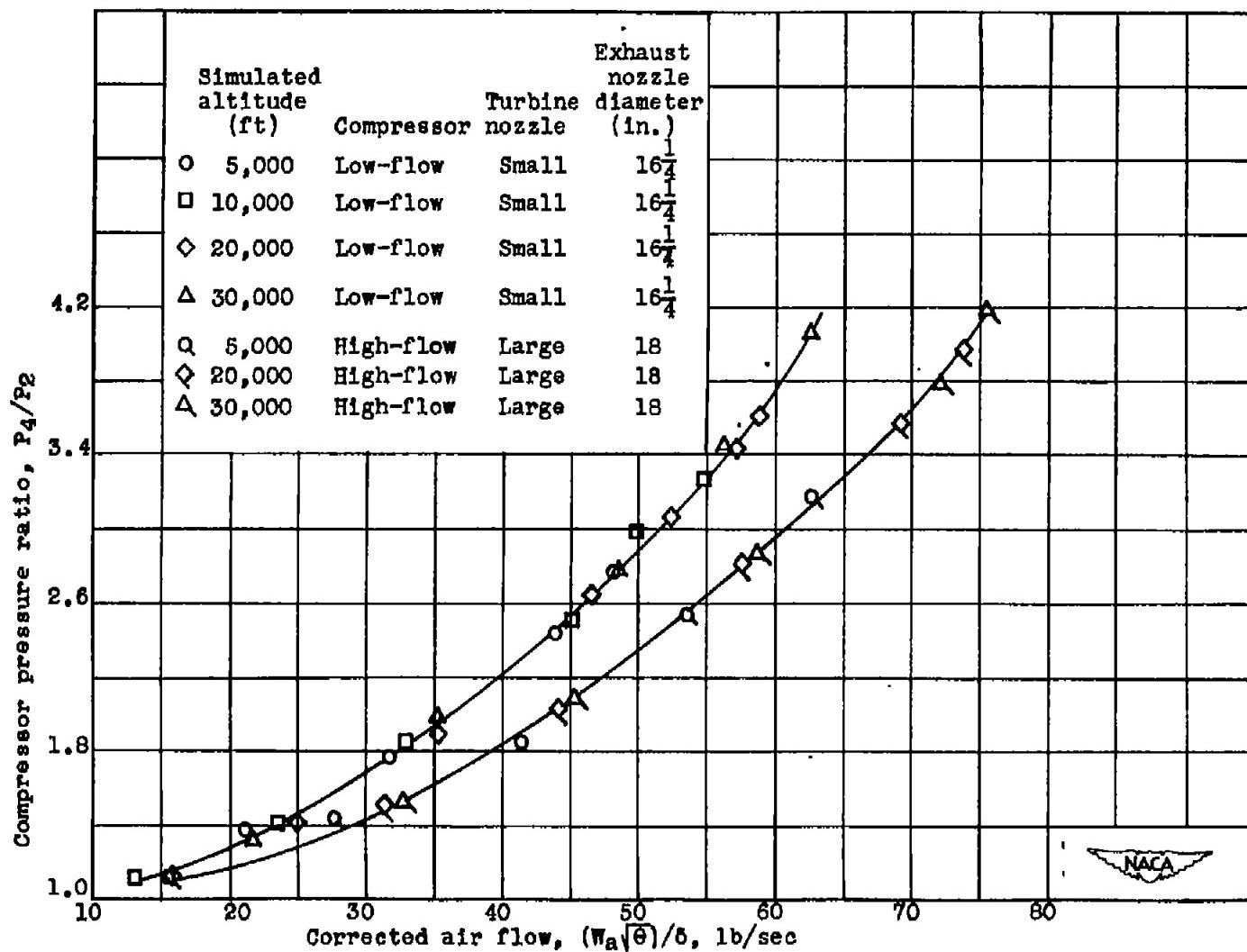
(a) Relation between compressor pressure ratio and corrected air flow.

Figure 10.- Effect of altitude on compressor operating line at static-test conditions.
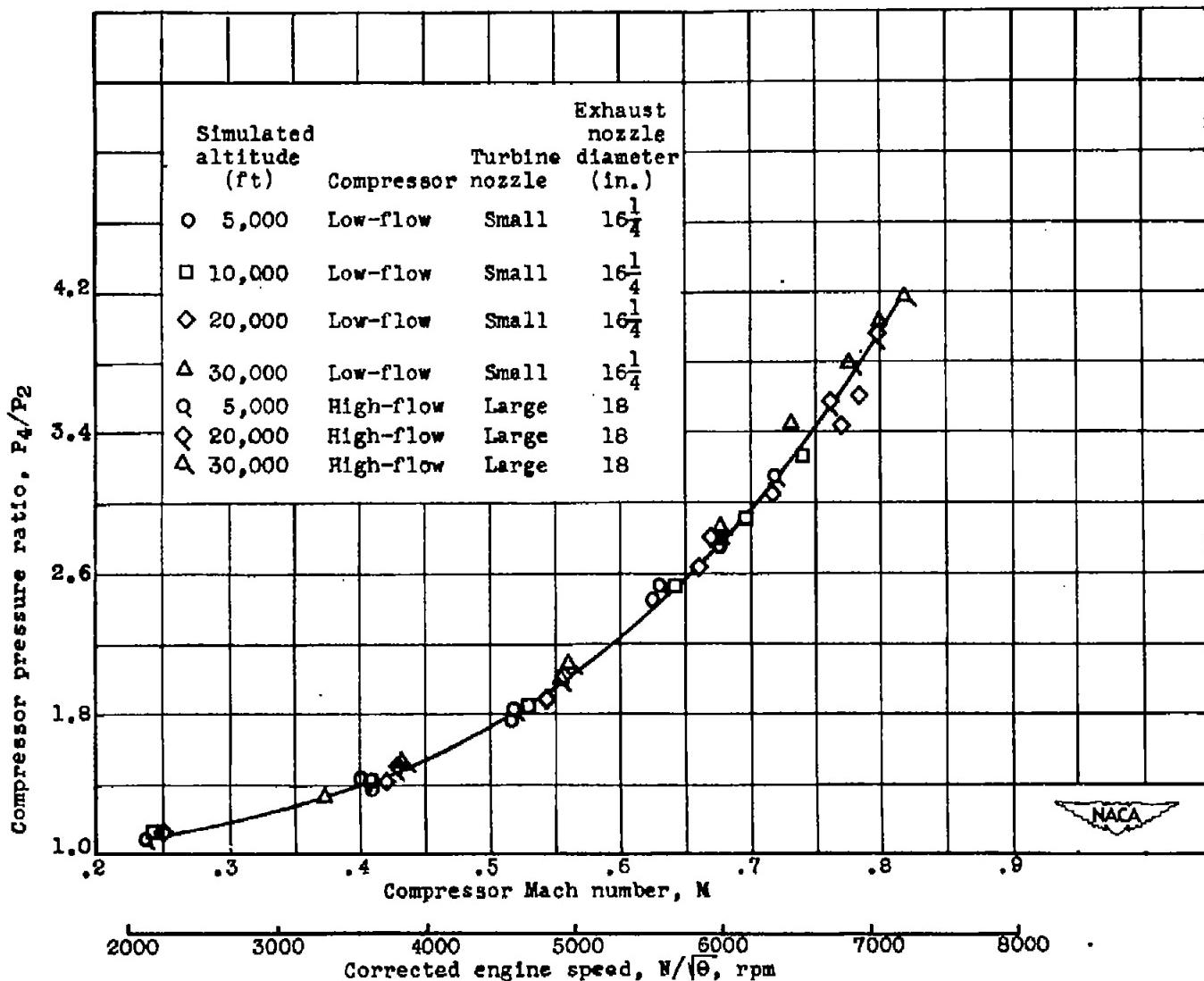
(b) Relation between compressor pressure ratio and compressor Mach number.
Figure 10.— Concluded.

	Approximate ram-pressure ratio, P_1/p_0	Compressor	Exhaust nozzle diameter (in.)
○	1.02	Low-flow	$16\frac{3}{4}$
□	1.20	Low-flow	$16\frac{3}{4}$
◇	1.41	Low-flow	$16\frac{3}{4}$
△	1.62	Low-flow	$16\frac{3}{4}$
▽	1.86	Low-flow	$16\frac{3}{4}$
◈	1.40	High-flow	18
▽	1.82	High-flow	18

High-flow compressor; ram-pressure ratio, 1.40 and 1.82

Low-flow compressor; ram-pressure ratio, 1.41, 1.62, and 1.86

Low-flow compressor; ram-pressure ratio, 1.20

Low-flow compressor; ram-pressure ratio, 1.02
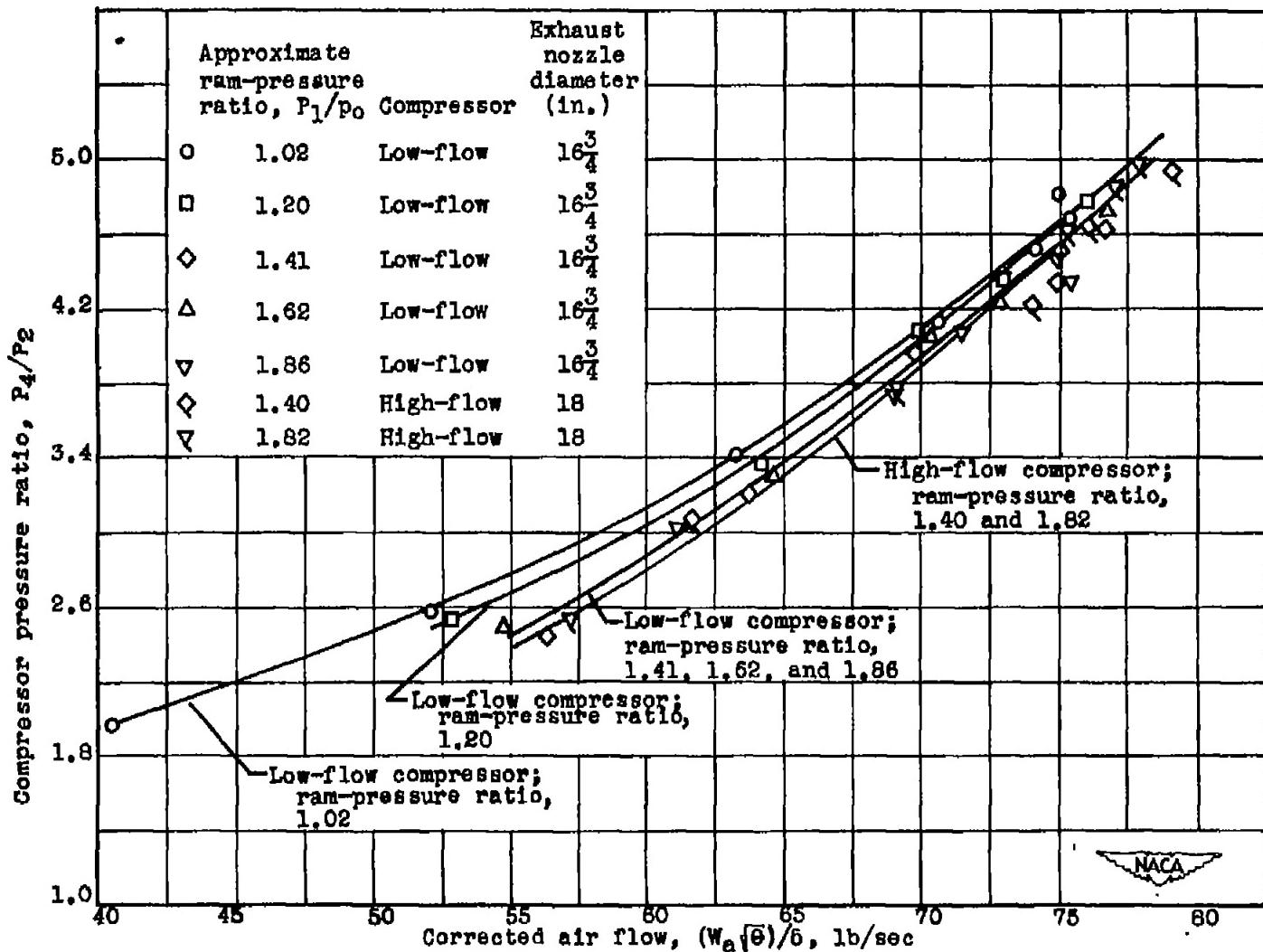
(a) Relation between compressor pressure ratio and corrected air flow.

Figure 11.— Effect of ram on compressor operating line. Simulated altitude, 40,000 feet; standard turbine nozzles.
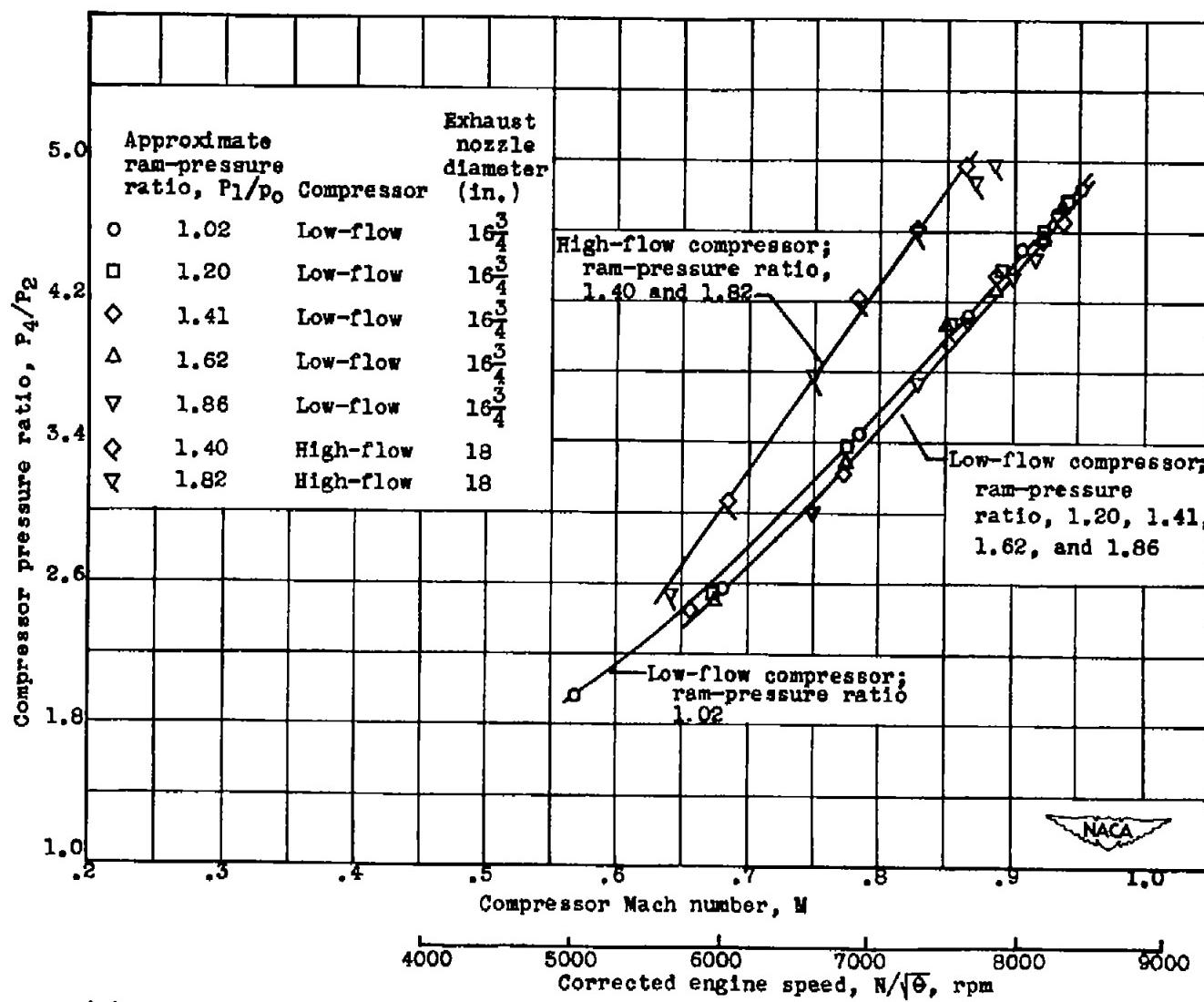
(b) Relation between compressor pressure ratio and compressor Mach number.

Figure 11.- Concluded.
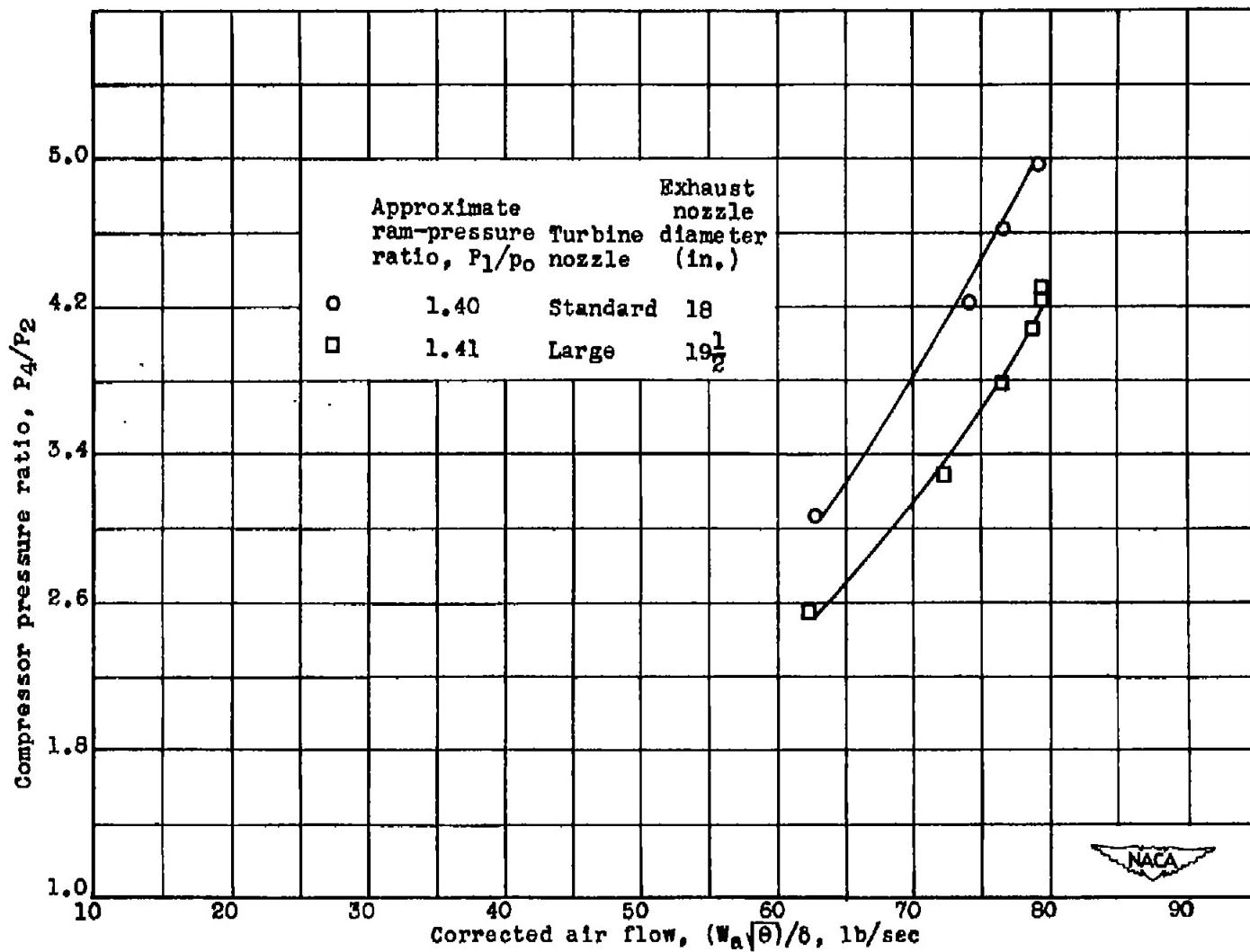
(a) Relation between compressor pressure ratio and corrected air flow.

Figure 12.- Effect of turbine nozzle area on compressor operating line. Simulated altitude, 40,000 feet; high-flow compressor.
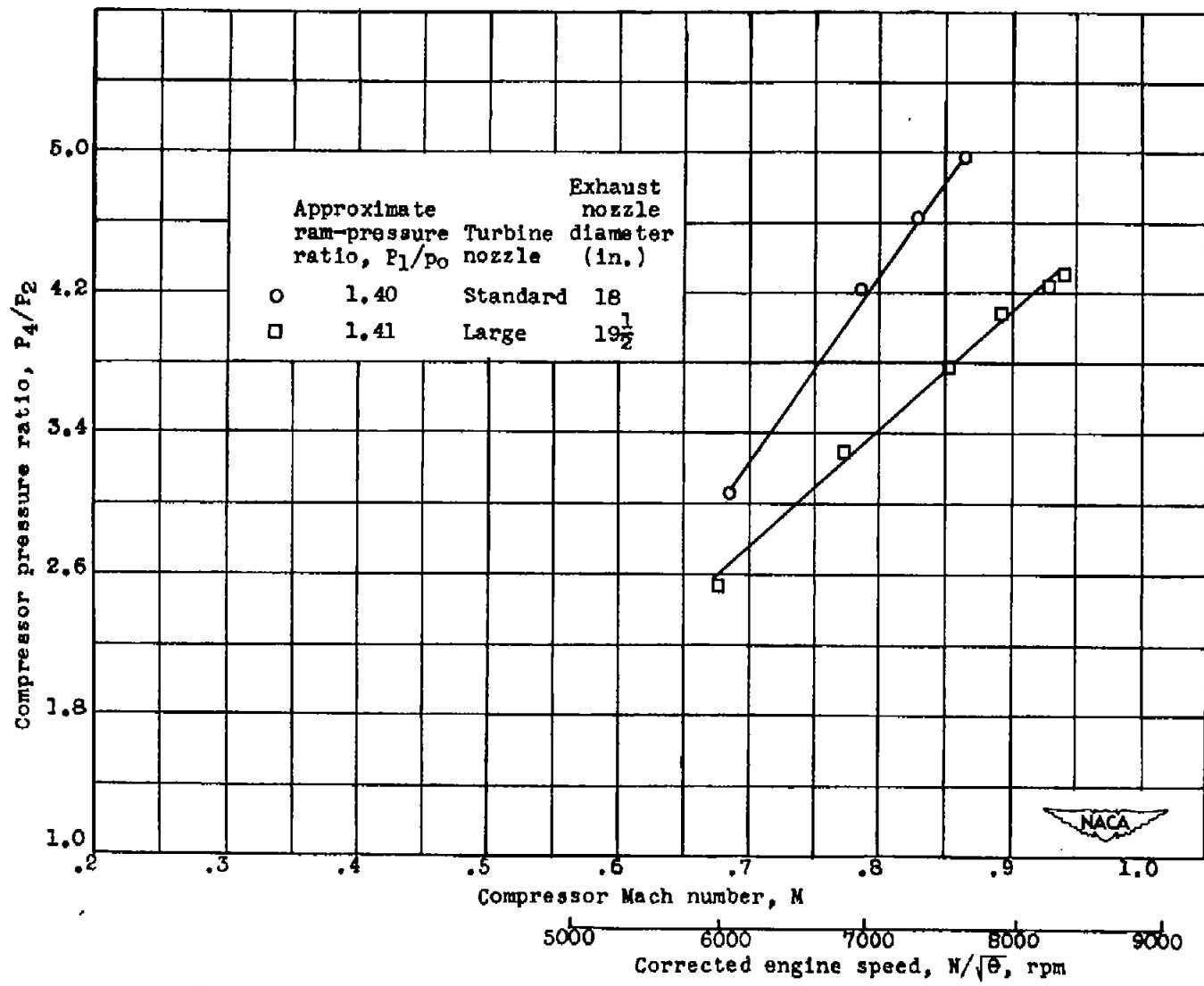
(b) Relation between compressor pressure ratio and compressor Mach number.
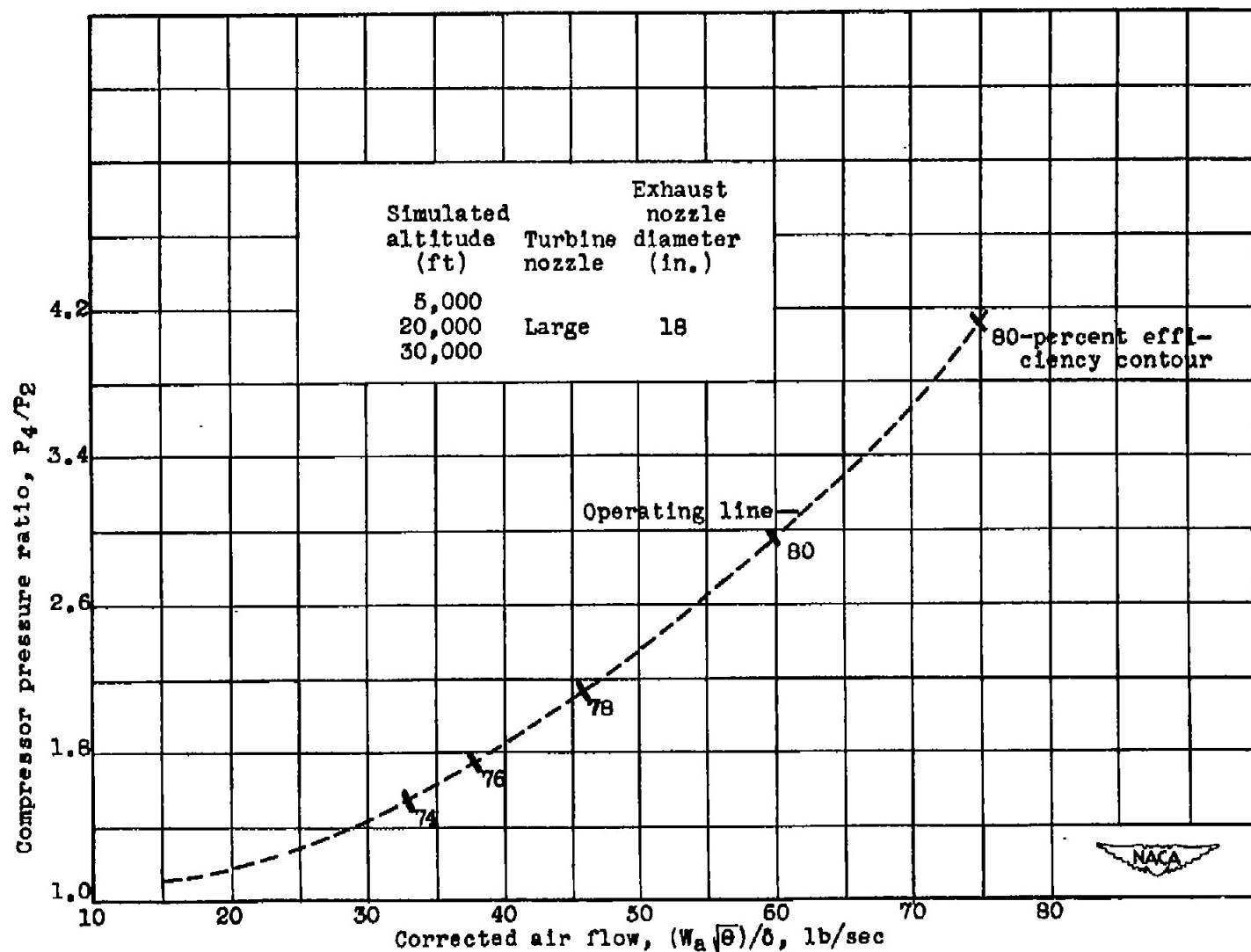
Figure 12.- Concluded.

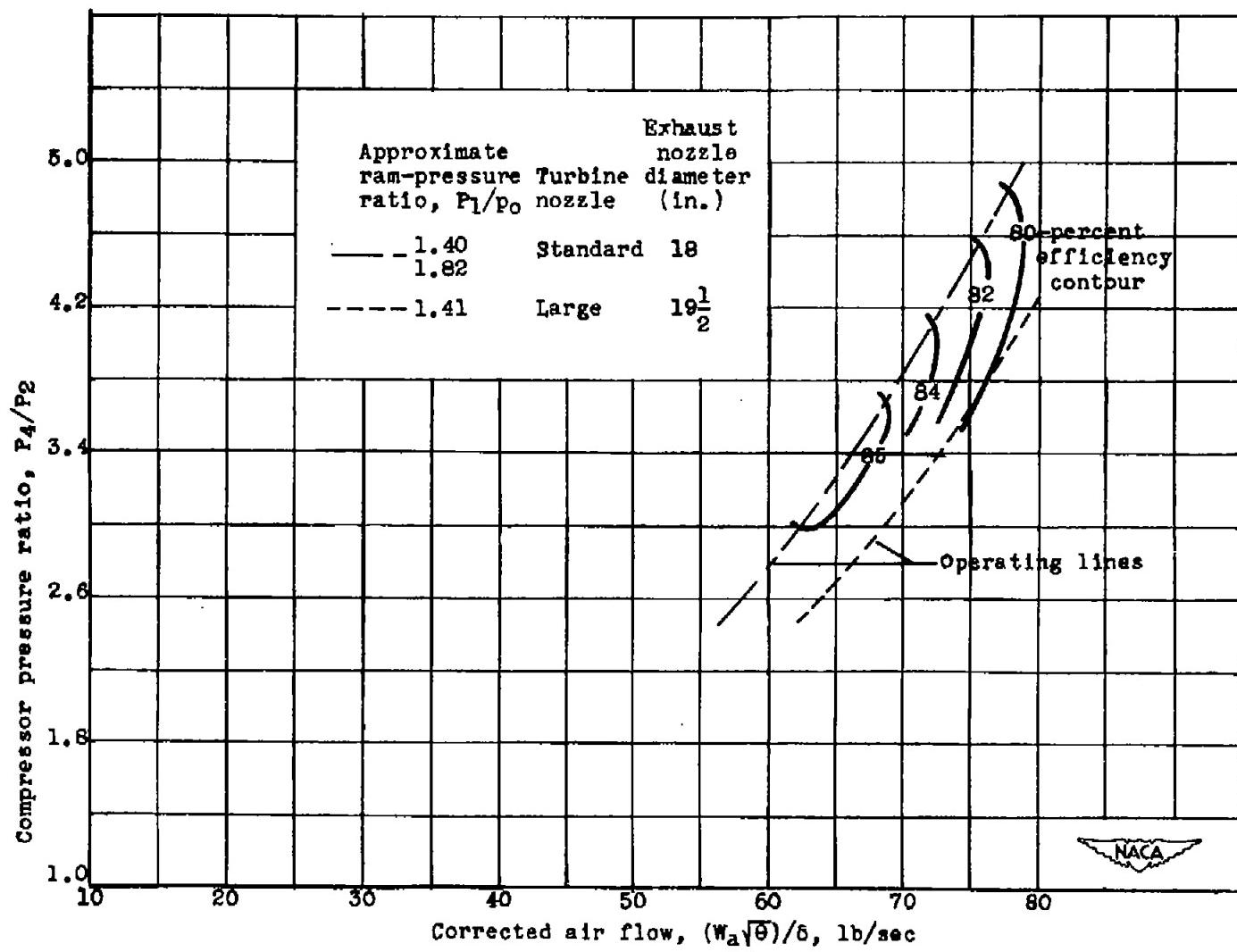(a) Static tests.

Figure 13.- Efficiency characteristics of low-flow compressor.
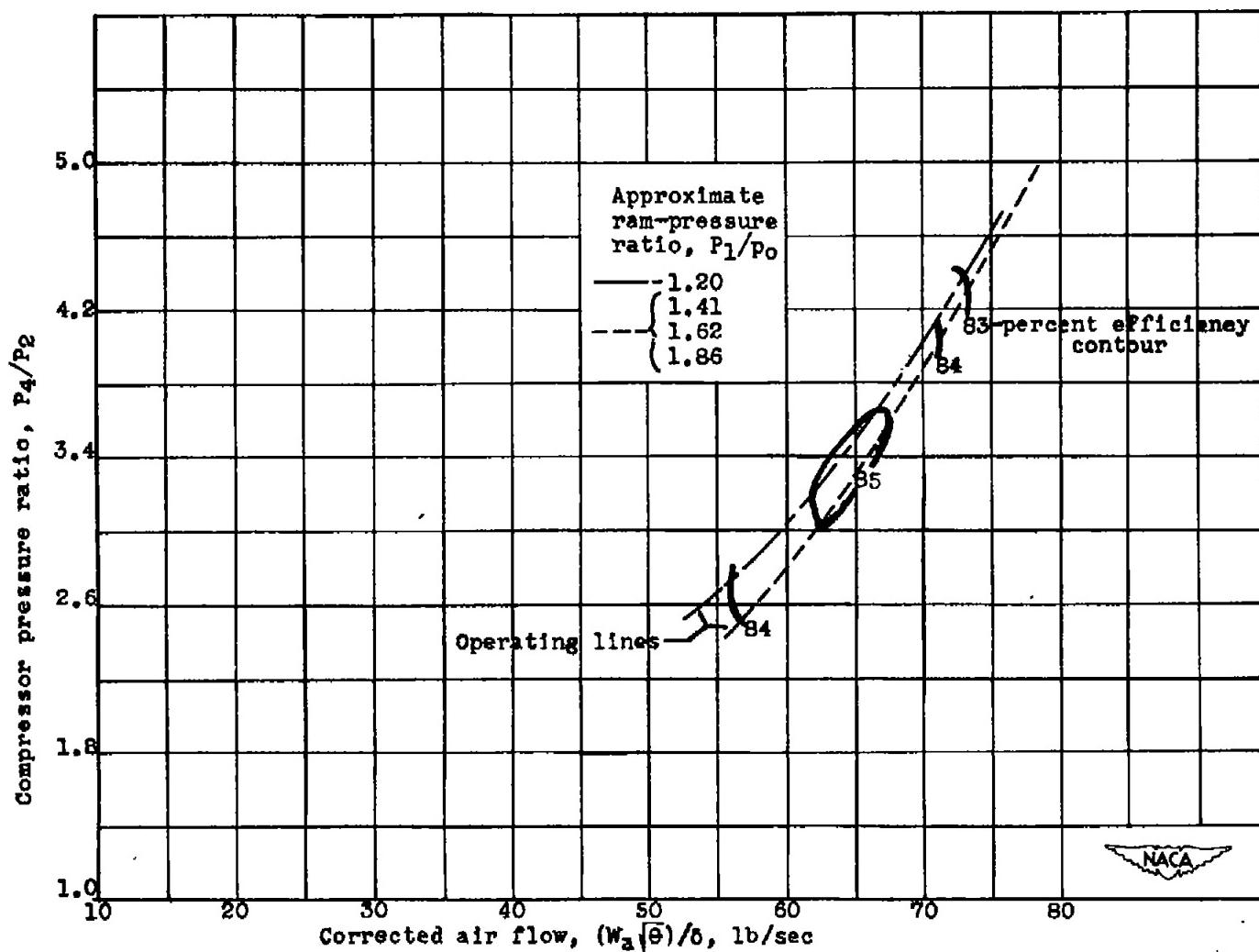
(b) Ram tests: Simulated altitude, 40,000 feet; standard turbine nozzle; exhaust-nozzle diameter, $16\frac{3}{4}$ inches.

Figure 13.- Concluded.

(a) Static tests.

Figure 14.- Efficiency characteristics of high-flow compressor.

(b) Ram tests: simulated altitude, 40,000 feet.

Figure 14.- Concluded.
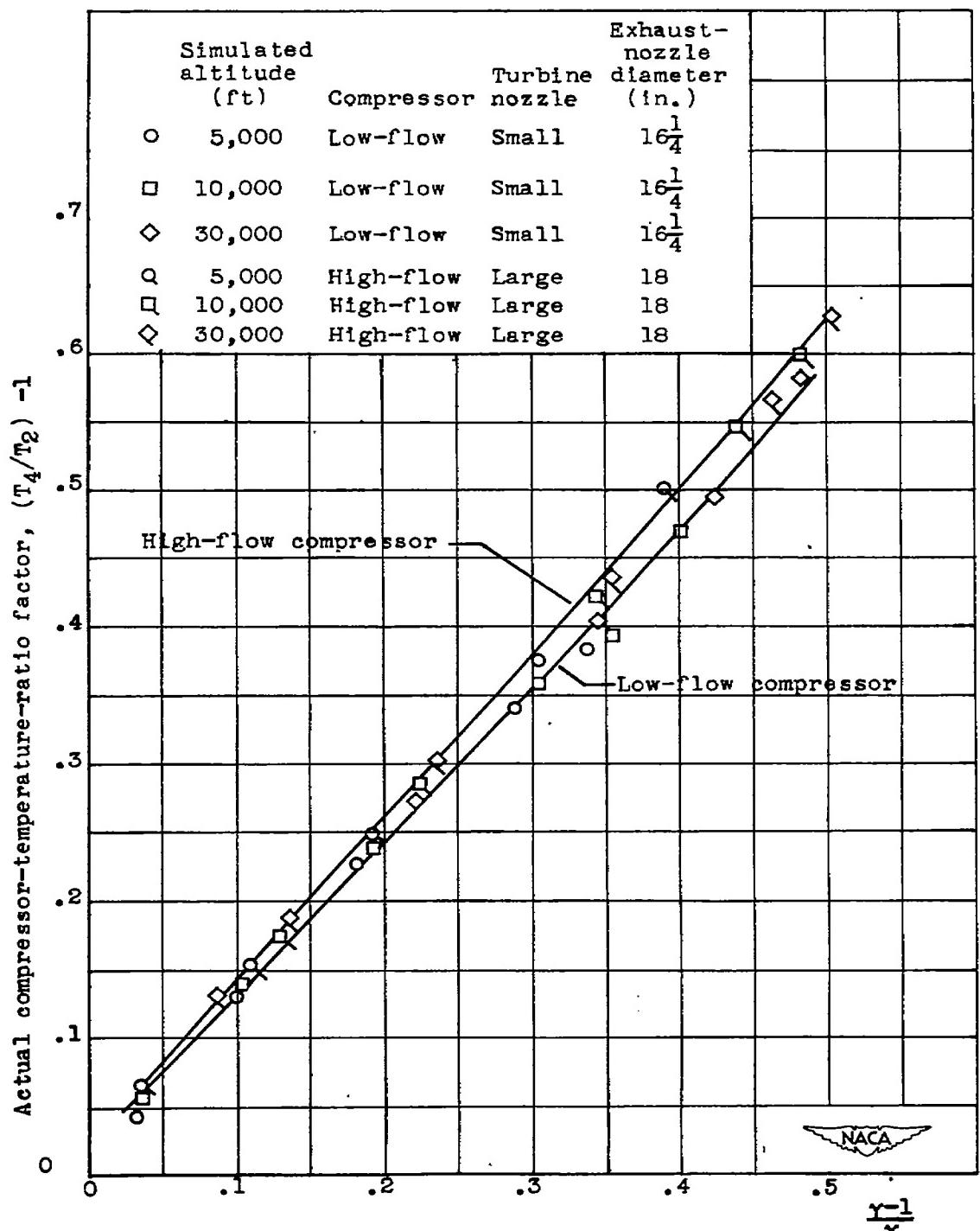
Figure 15.- Effect of altitude on relation of actual to adiabatic temperature-rise ratio across compressor at static-test conditions.
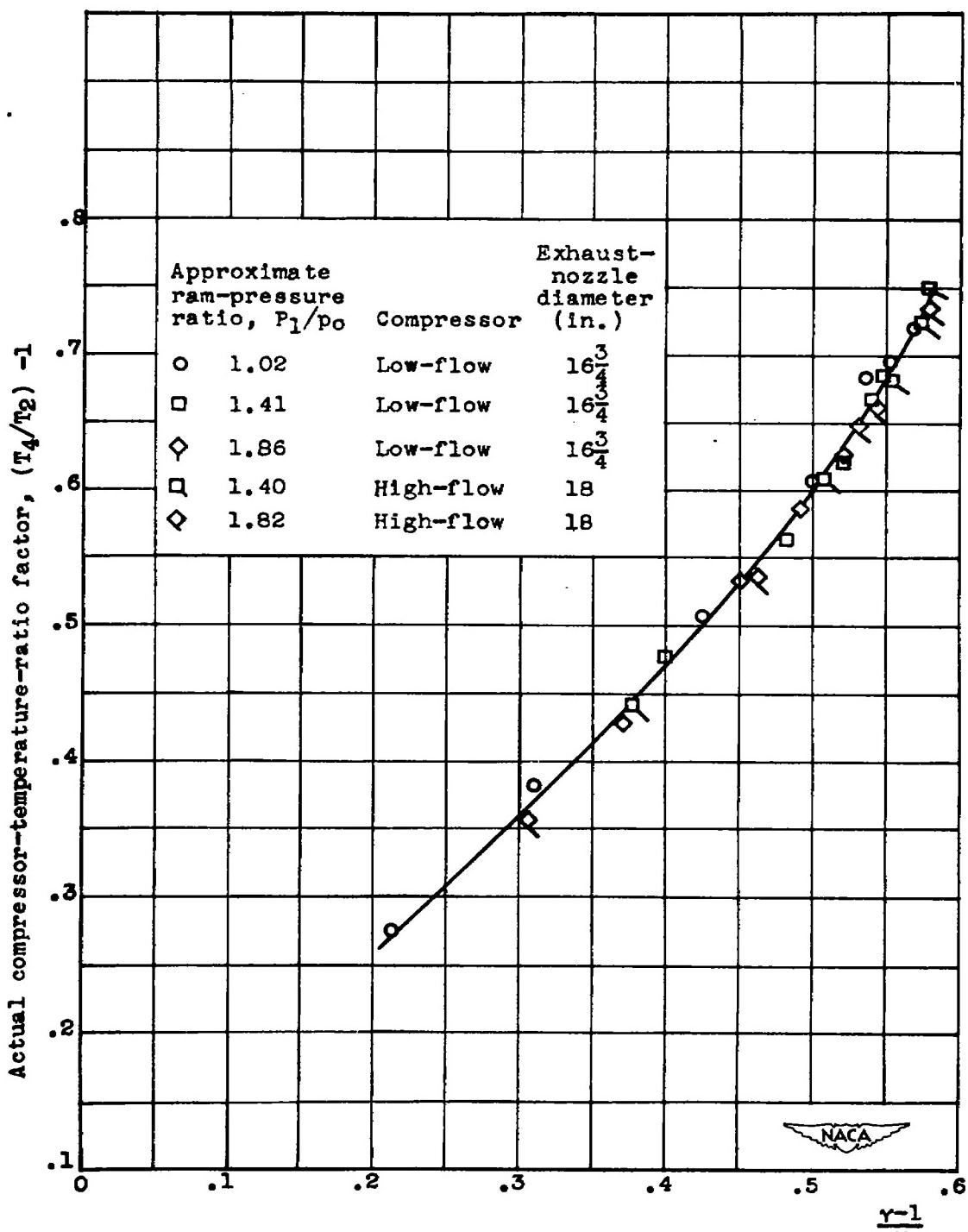
Figure 16.- Effect of ram on relation of actual to adiabatic temperature-rise ratio across compressor. Simulated altitude, 40,000 feet; standard turbine nozzle.
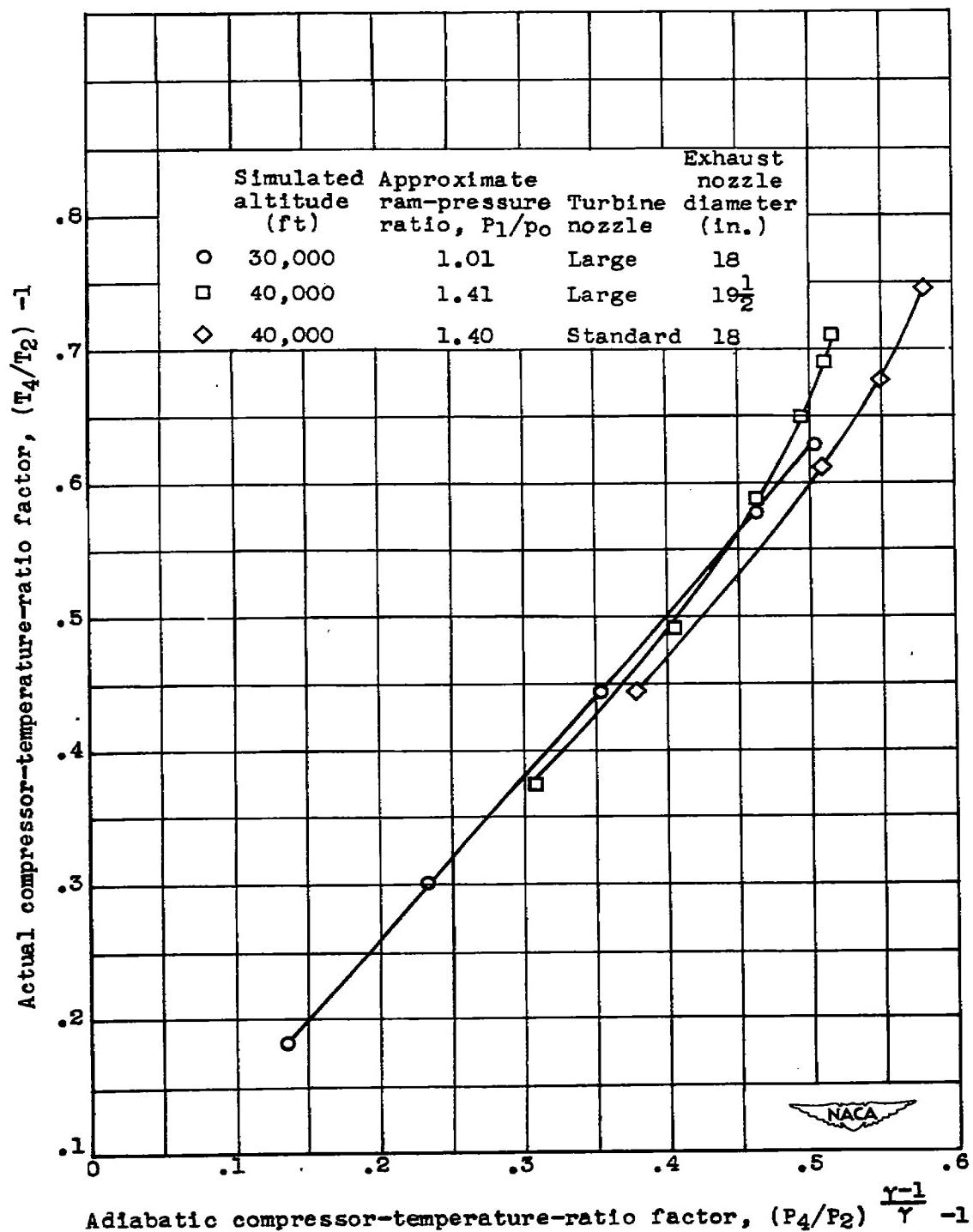
	Simulated altitude (ft)	Approximate ram-pressure ratio, P_1/p_0	Turbine nozzle	Exhaust nozzle diameter (in.)
○	30,000	1.01	Large	18
□	40,000	1.41	Large	$19\frac{1}{2}$
◇	40,000	1.40	Standard	18

Actual compressor-temperature-ratio factor, $(T_4/T_2) -1$

Adiabatic compressor-temperature-ratio factor, $(P_4/P_2)^{\frac{\gamma-1}{\gamma}} -1$

Figure 17.- Effect of turbine nozzle area on relation of actual to adiabatic temperature-rise ratio across high-flow compressor.
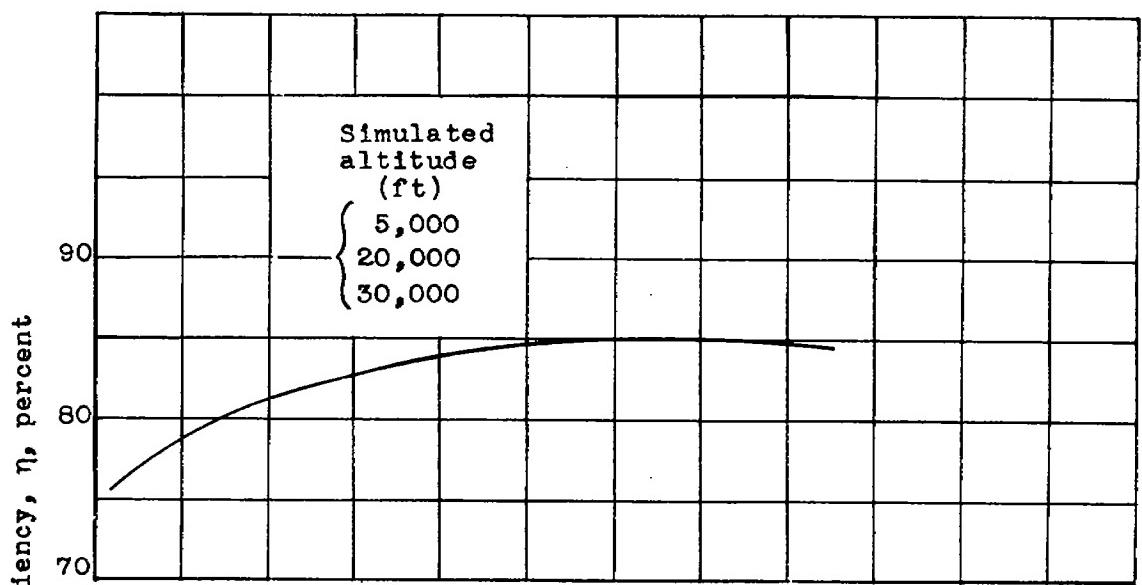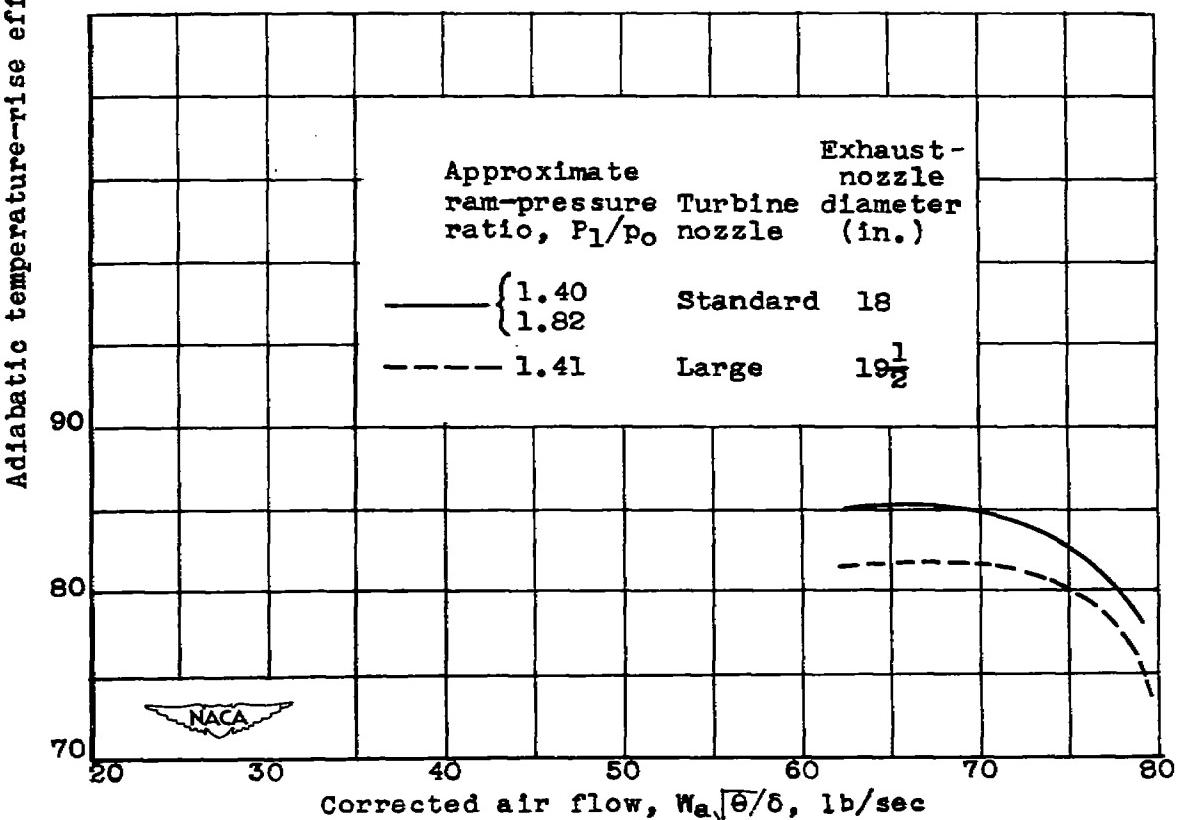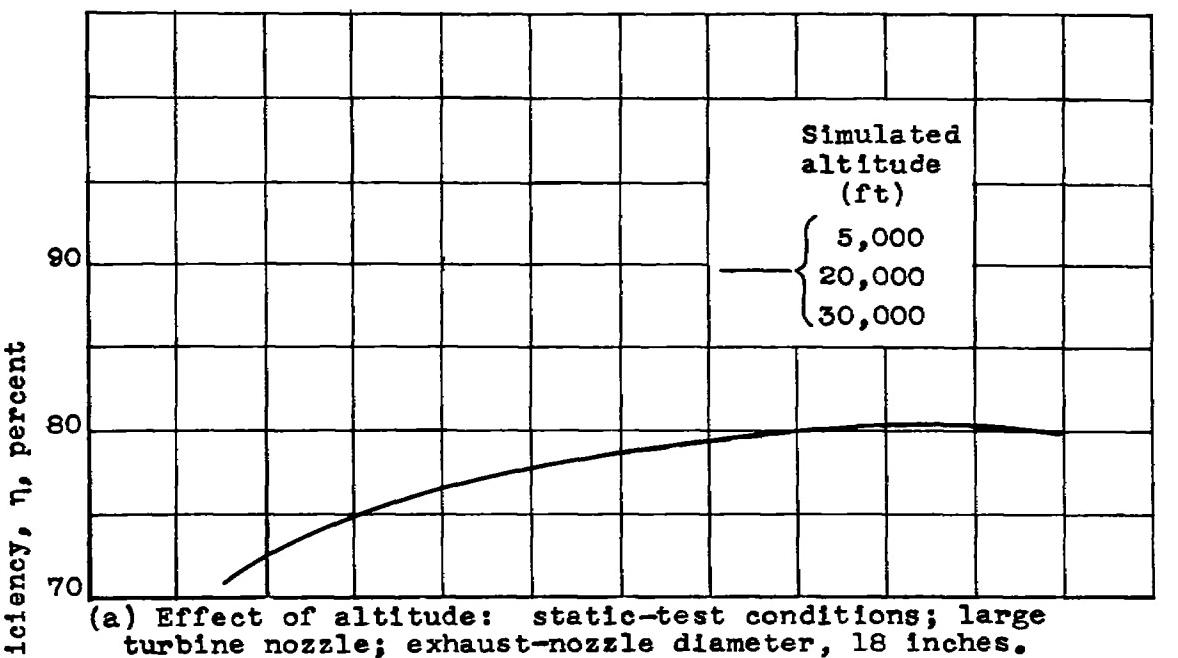
(a) Effect of altitude at static-test conditions: exhaust-
     nozzle diameter, $16\frac{1}{4}$ inches; small turbine nozzle.
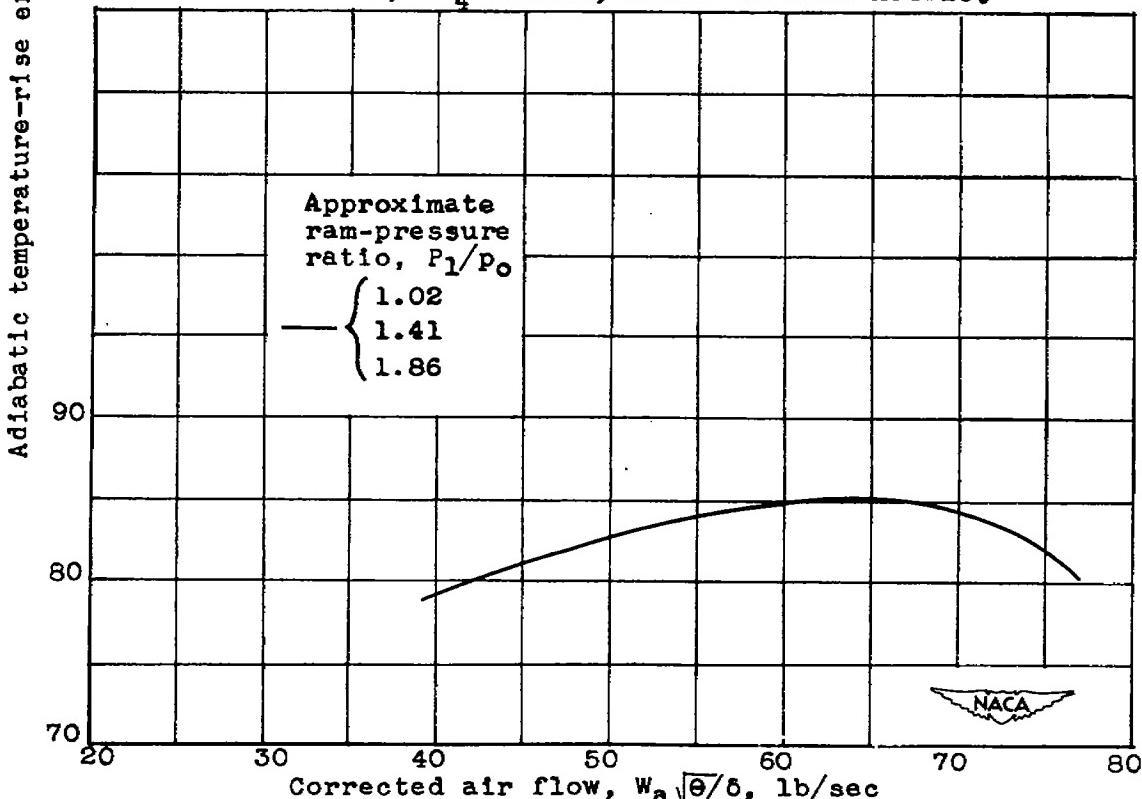
(b) Effect of ram: simulated altitude, 40,000 feet; exhaust-
     nozzle diameter, $16\frac{3}{4}$ inches; standard turbine nozzle.

Figure 18.— Low-flow compressor efficiencies.

582

(a) Effect of altitude: static-test conditions; large
turbine nozzle; exhaust-nozzle diameter, 18 inches.

(b) Effect of ram: simulated altitude, 40,000 feet.

Figure 19.- High-flow compressor efficiencies.

(a) Low-flow compressor; small turbine nozzle; exhaust-nozzle diameter, $16\frac{1}{4}$ inches.

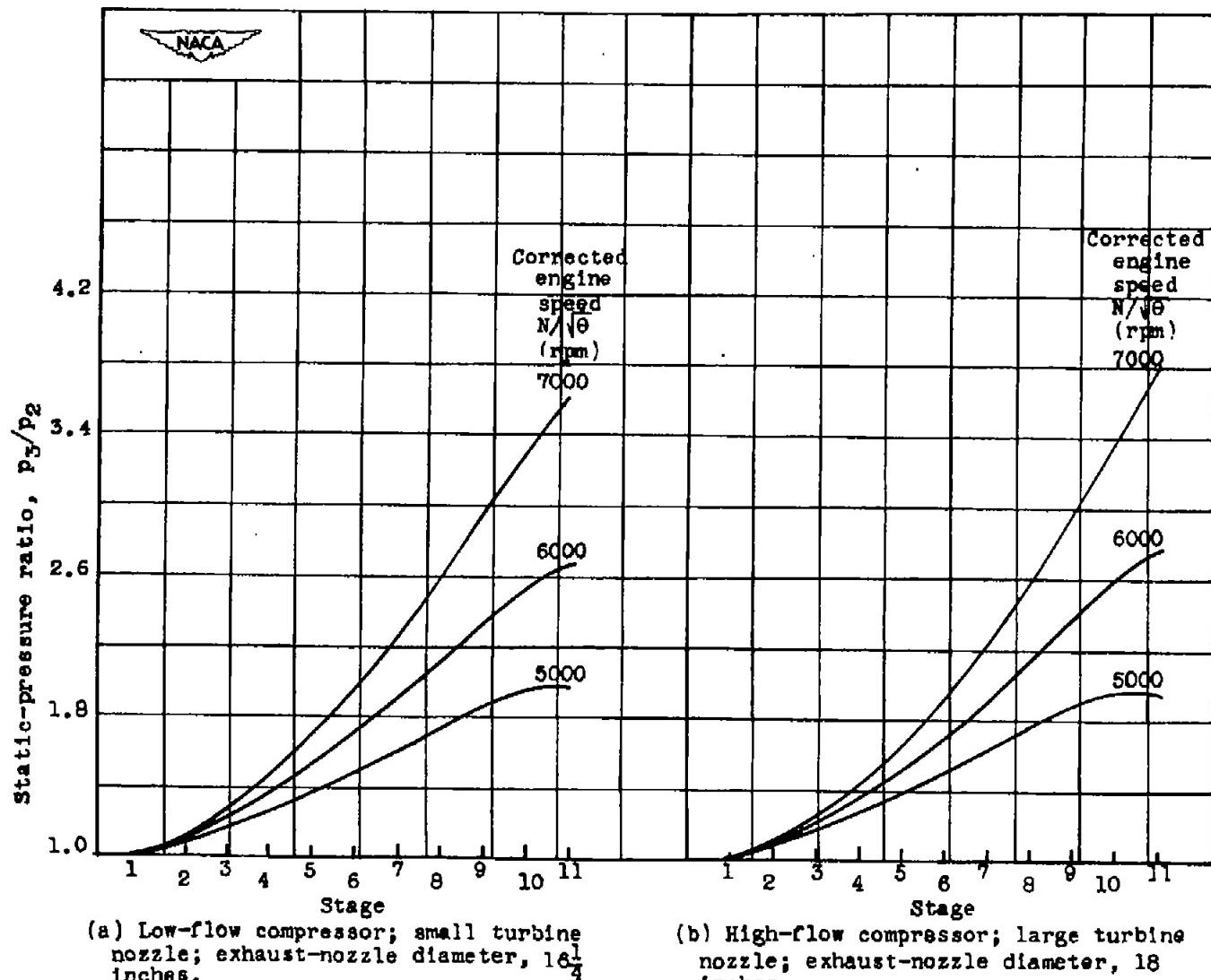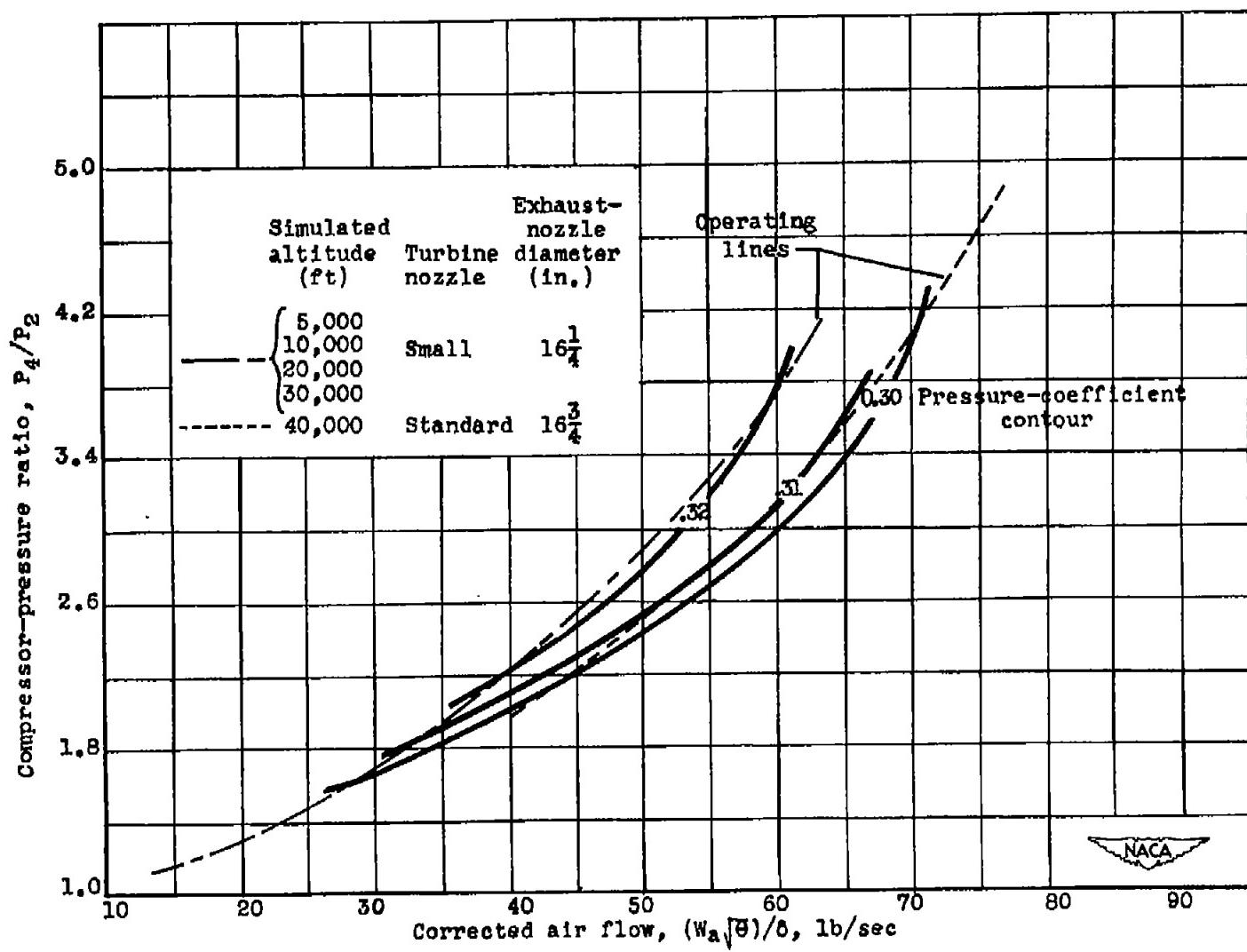(b) High-flow compressor; large turbine nozzle; exhaust-nozzle diameter, 18 inches.
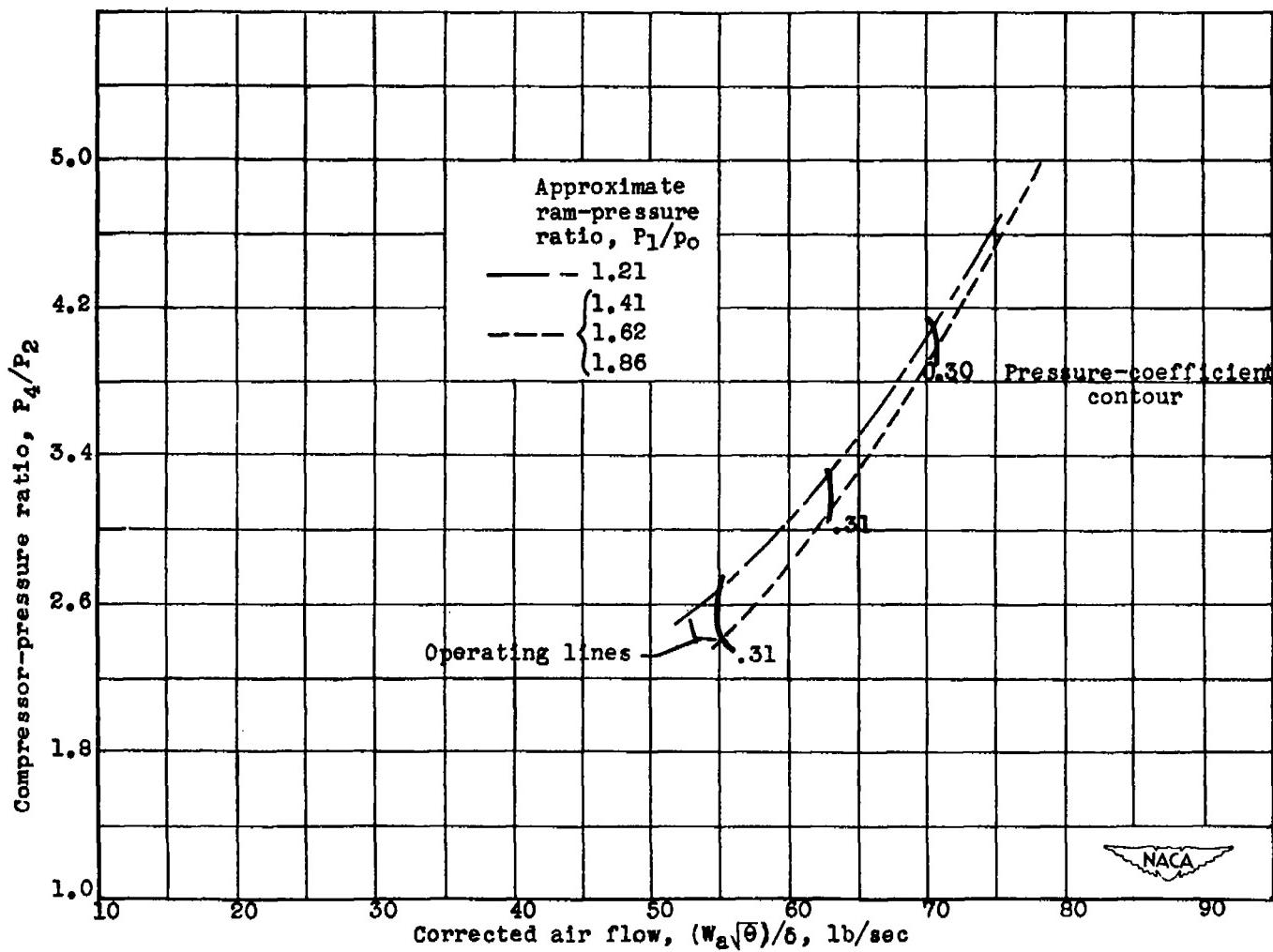
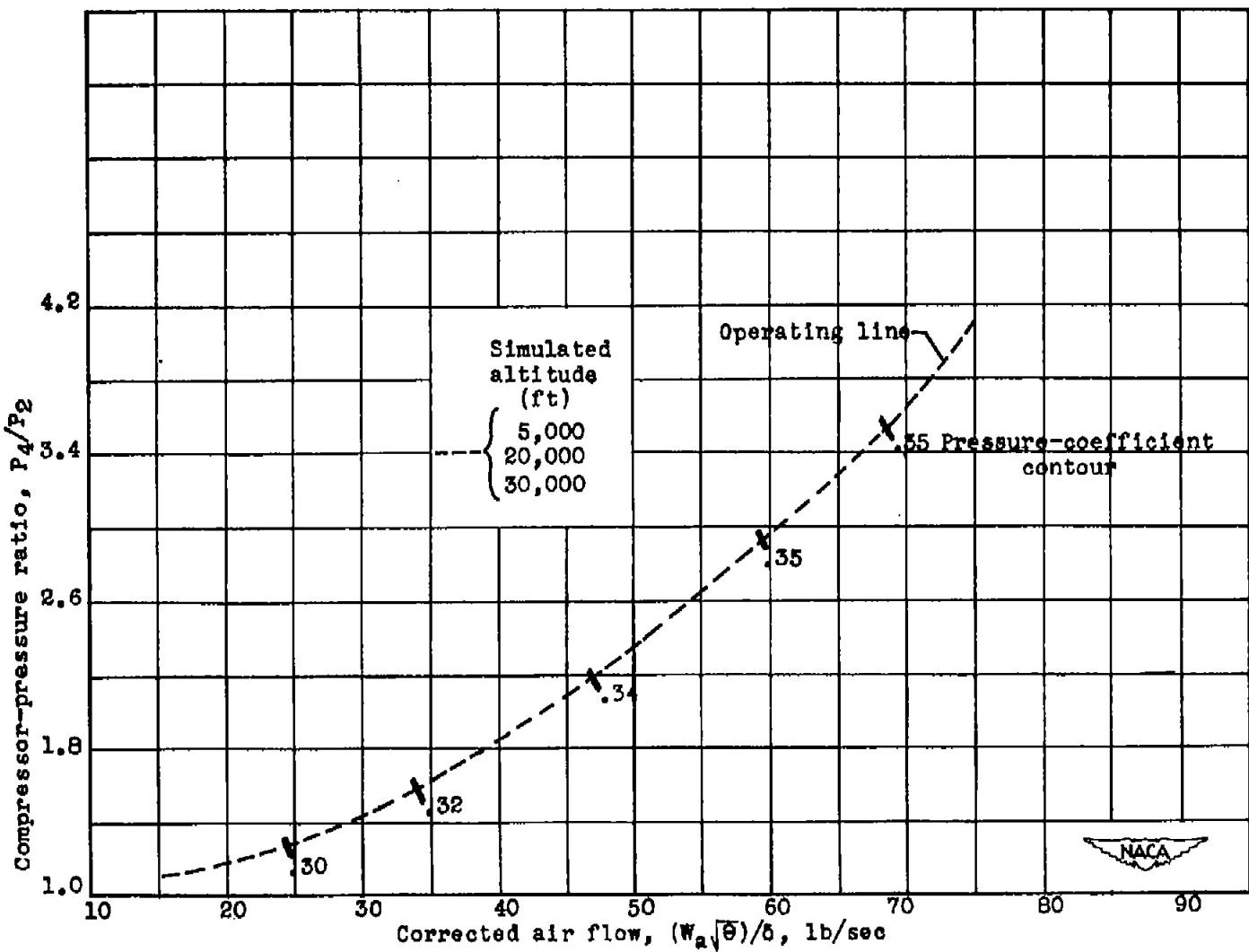Figure 20.- Compressor interstage pressures at static-test conditions.

(a) Static tests.

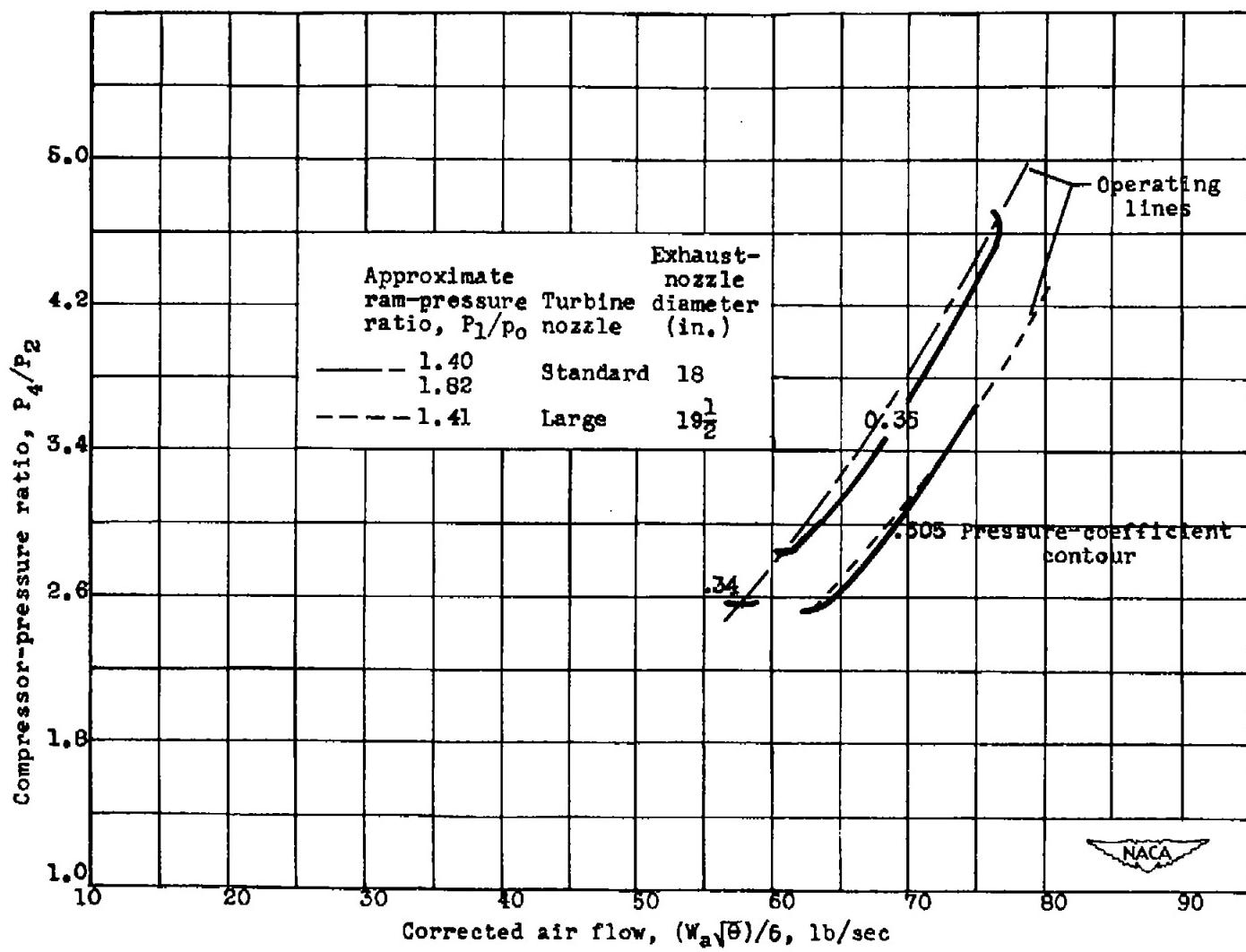Figure 21.- Pressure-coefficient contours for low-flow compressor.

(b) Ram tests: simulated altitude, 40,000 feet; standard turbine nozzle; exhaust-nozzle diameter, $16\frac{3}{4}$ inches.

Figure 21.- Concluded.

(a) Static tests: large turbine nozzle; exhaust-nozzle diameter, 18 inches.

Figure 22.- Pressure-coefficient contours for high-flow compressor.

(b) Ram tests: simulated altitude, 40,000 feet.

Figure 22.- Concluded.

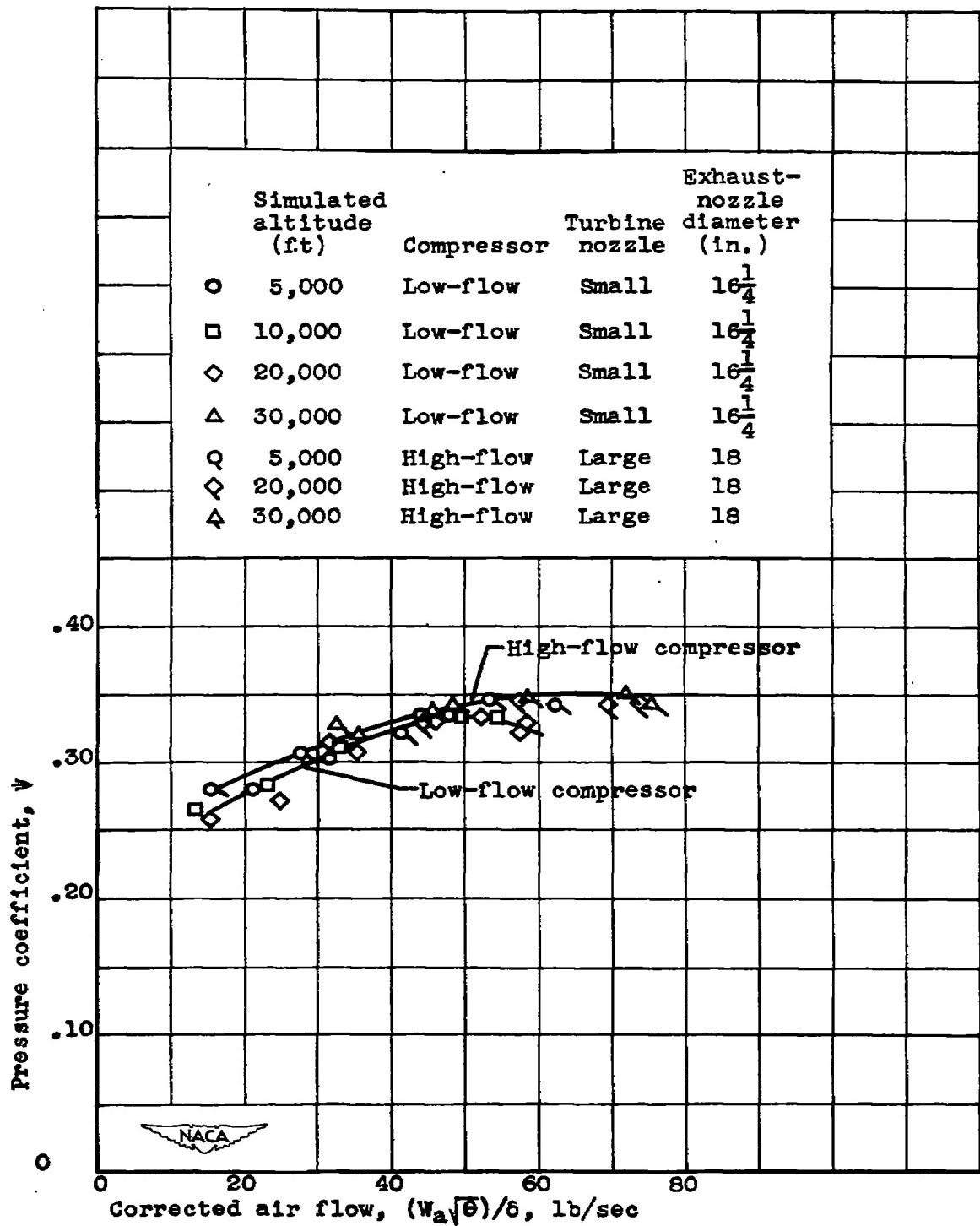|	Simulated altitude (ft)	Compressor	Turbine nozzle	Exhaust-nozzle diameter (in.)
O	5,000	Low-flow	Small	$16\frac{1}{4}$
□	10,000	Low-flow	Small	$16\frac{1}{4}$
◇	20,000	Low-flow	Small	$16\frac{1}{4}$
△	30,000	Low-flow	Small	$16\frac{1}{4}$
Q	5,000	High-flow	Large	18
◇	20,000	High-flow	Large	18
△	30,000	High-flow	Large	18

Figure 23.— Effect of altitude on relation between compressor-pressure coefficients and corrected air flow through compressor at static-test conditions.
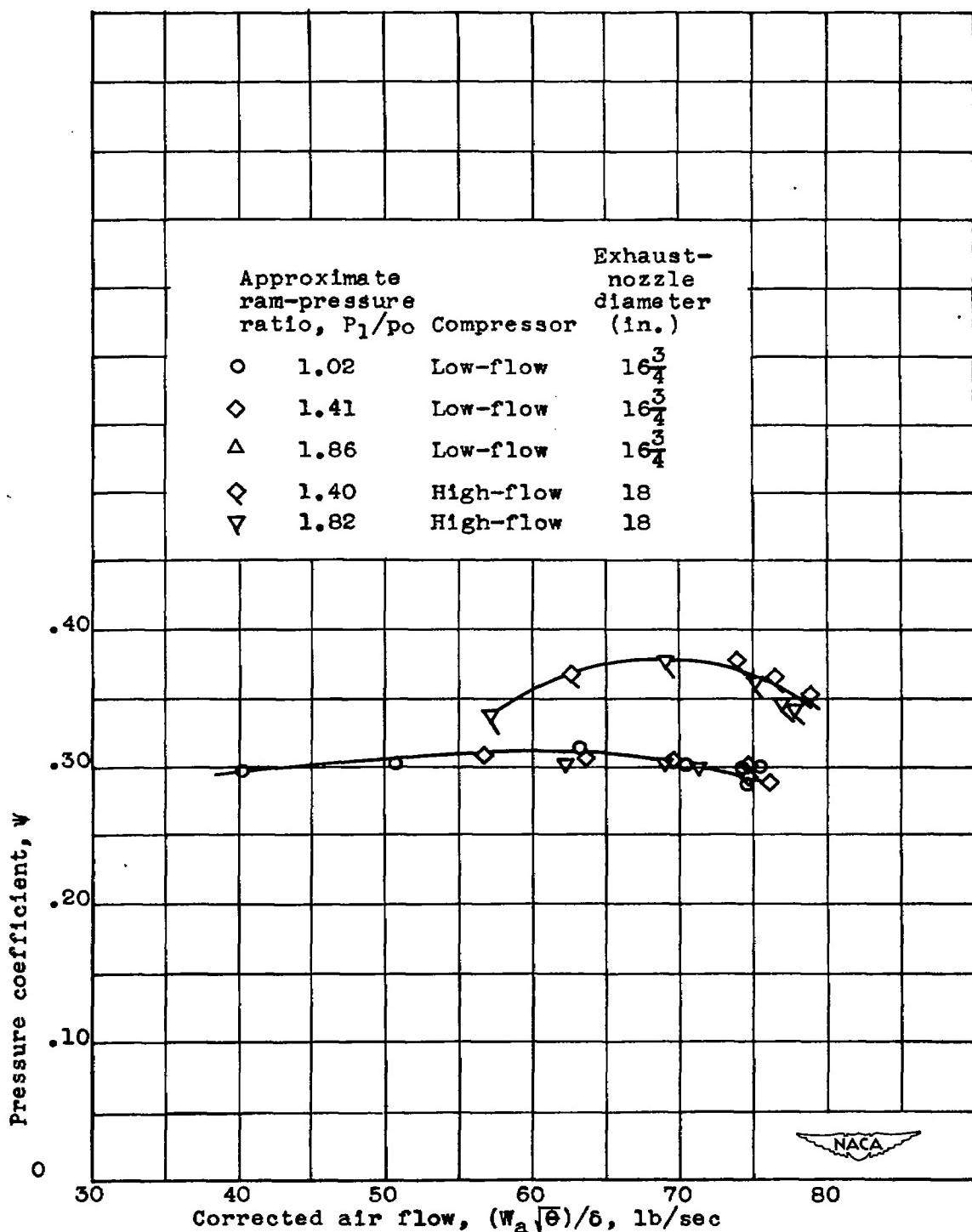
Approximate ram-pressure ratio, P_1/p_0	Compressor	Exhaust-nozzle diameter (in.)
○ 1.02	Low-flow	$16\frac{3}{4}$
◇ 1.41	Low-flow	$16\frac{3}{4}$
△ 1.86	Low-flow	$16\frac{3}{4}$
◈ 1.40	High-flow	18
▽ 1.82	High-flow	18

Figure 24.- Effect of ram on relation between compressor-pressure coefficients and corrected air flow through compressor. Simulated altitude, 40,000 feet; standard turbine nozzle.
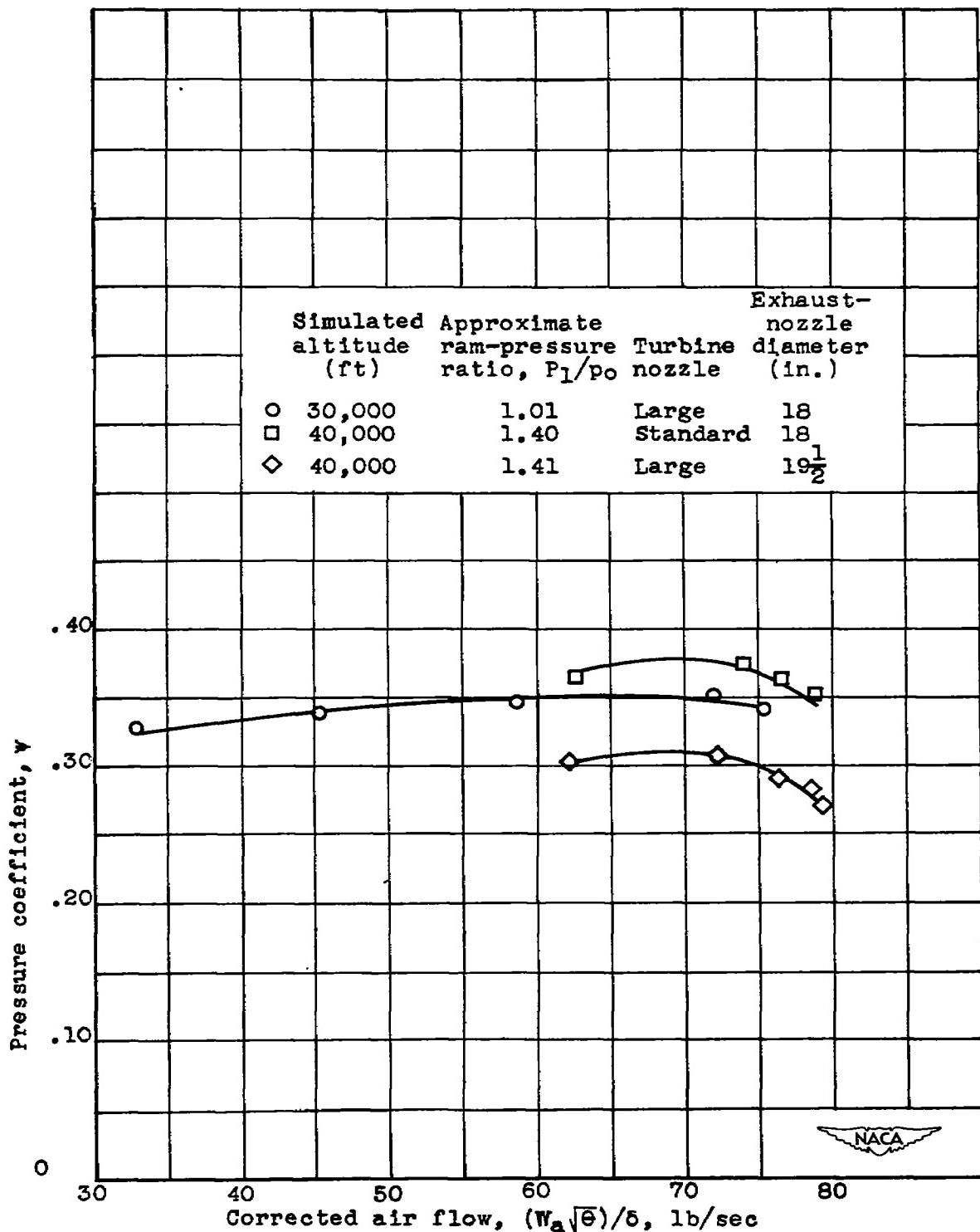
582

	Simulated altitude (ft)	Approximate ram-pressure ratio, P_1/p_0	Turbine nozzle	Exhaust-nozzle diameter (in.)
O	30,000	1.01	Large	18
□	40,000	1.40	Standard	18
◇	40,000	1.41	Large	$19\frac{1}{2}$

Pressure coefficient, ψ

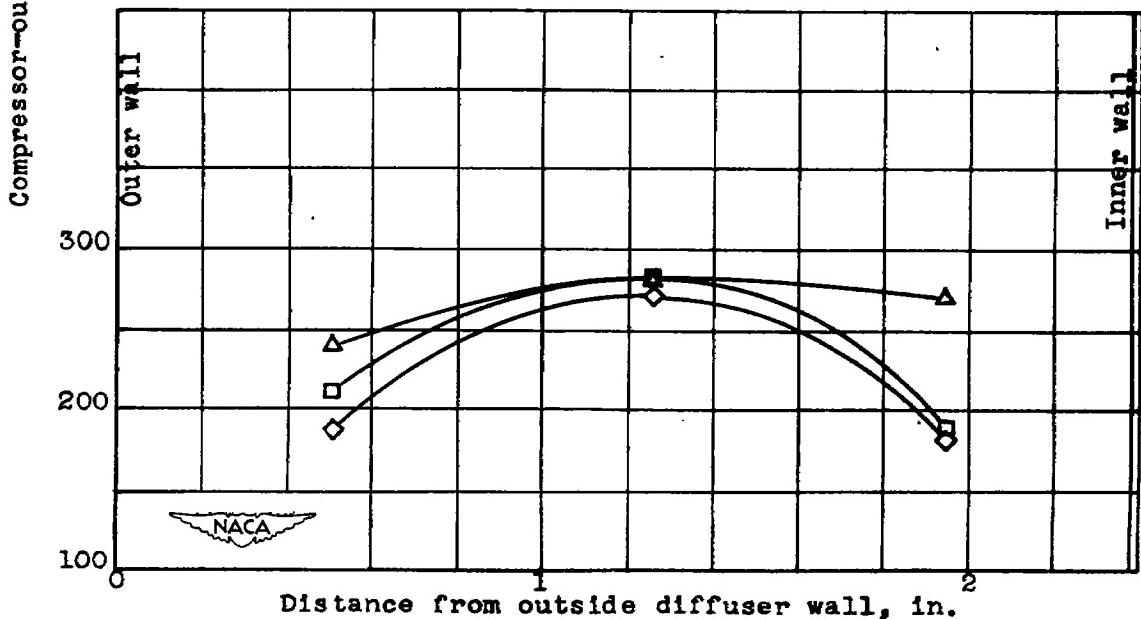Corrected air flow, $(W_a\sqrt{\theta})/\delta$, lb/sec

Figure 25.- Effect of turbine-nozzle area on relation between compressor-pressure coefficients and corrected air flow through high-flow compressor.
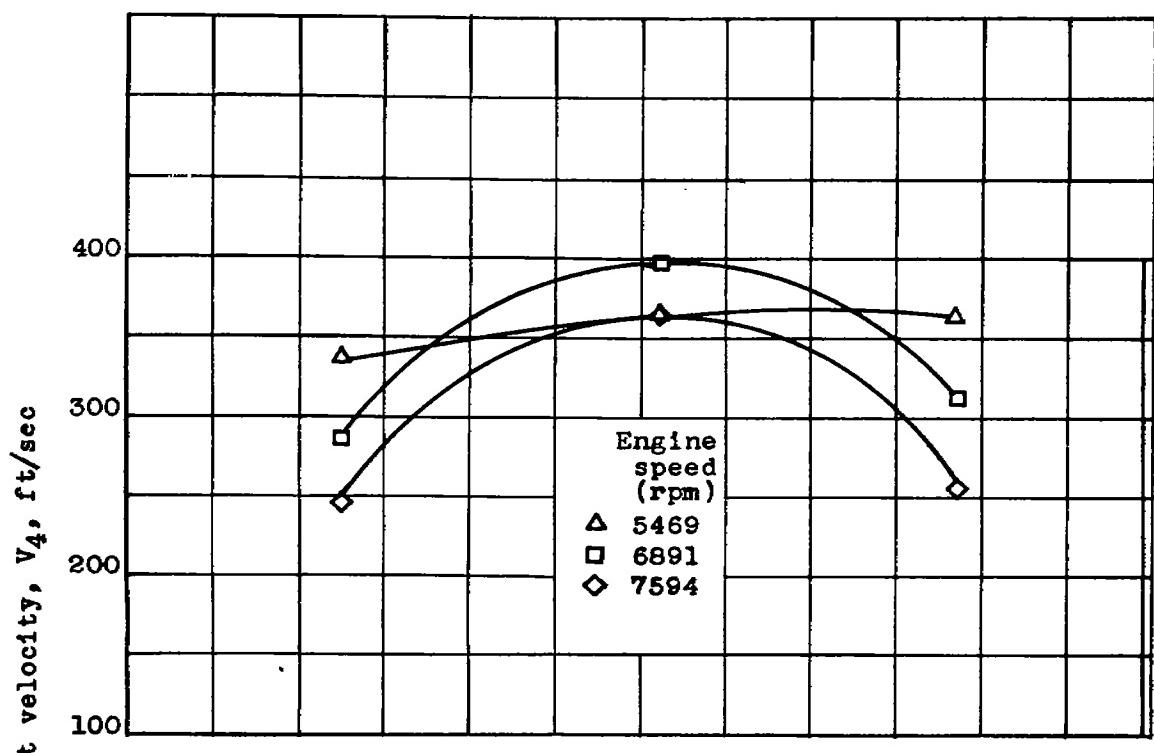
(a) Simulated altitude, 10,000 feet; ram-pressure ratio, 1.21.

Engine
speed
(rpm)
△ 5469
□ 6891
◇ 7594

Distance from outside diffuser wall, in.

(b) Simulated altitude, 40,000 feet; ram-pressure ratio, 1.20.

Figure 26.- Velocity profile at outlet of low-flow compressor.
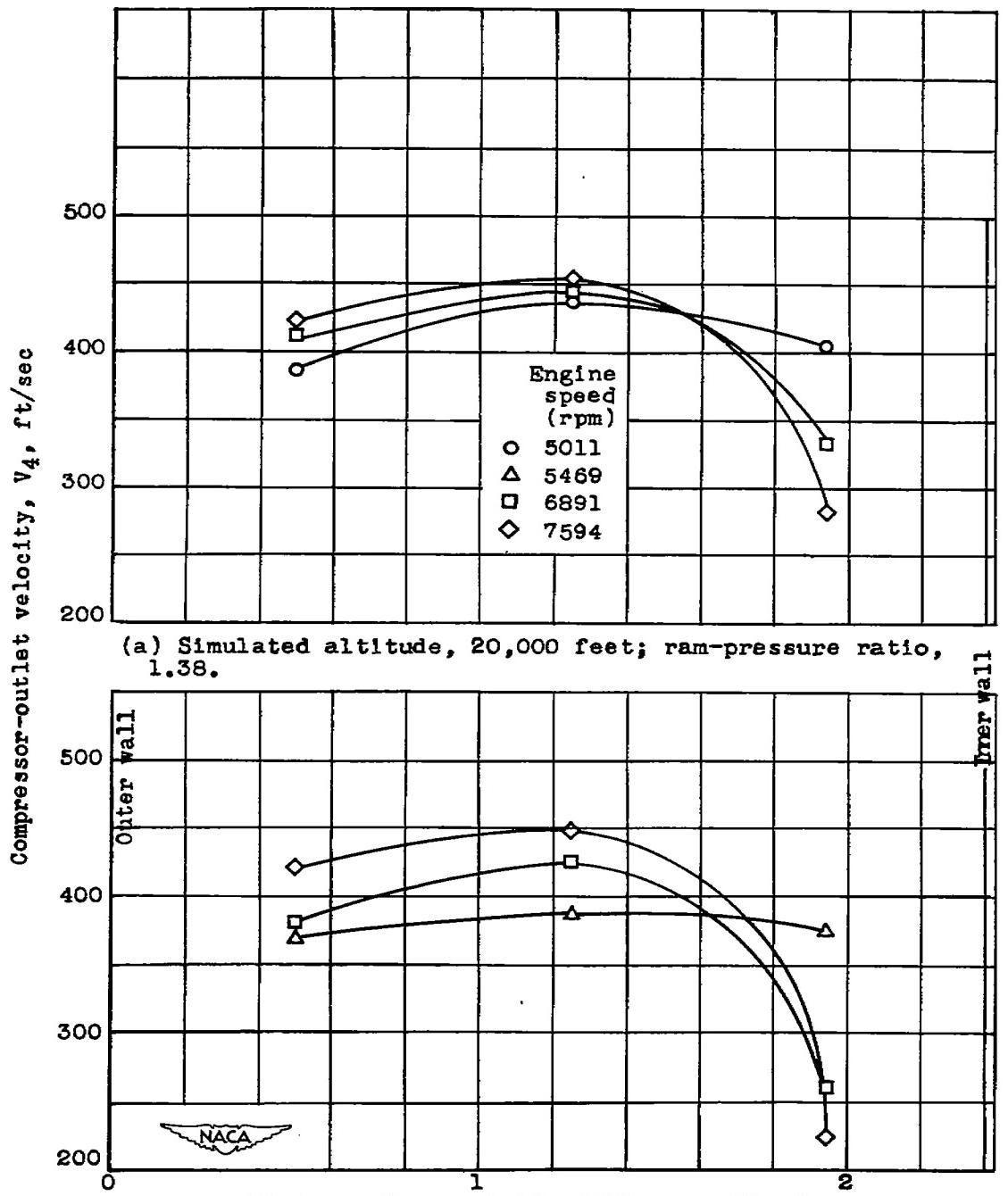Standard turbine nozzle; exhaust-nozzle diameter, $16\frac{3}{4}$
inches.

582

(a) Simulated altitude, 20,000 feet; ram-pressure ratio, 1.38.

(b) Simulated altitude, 40,000 feet; ram-pressure ratio, 1.40.

Figure 27.- Velocity profile at outlet of high-flow compressor. Standard turbine nozzle; exhaust-nozzle diameter, 18 inches.
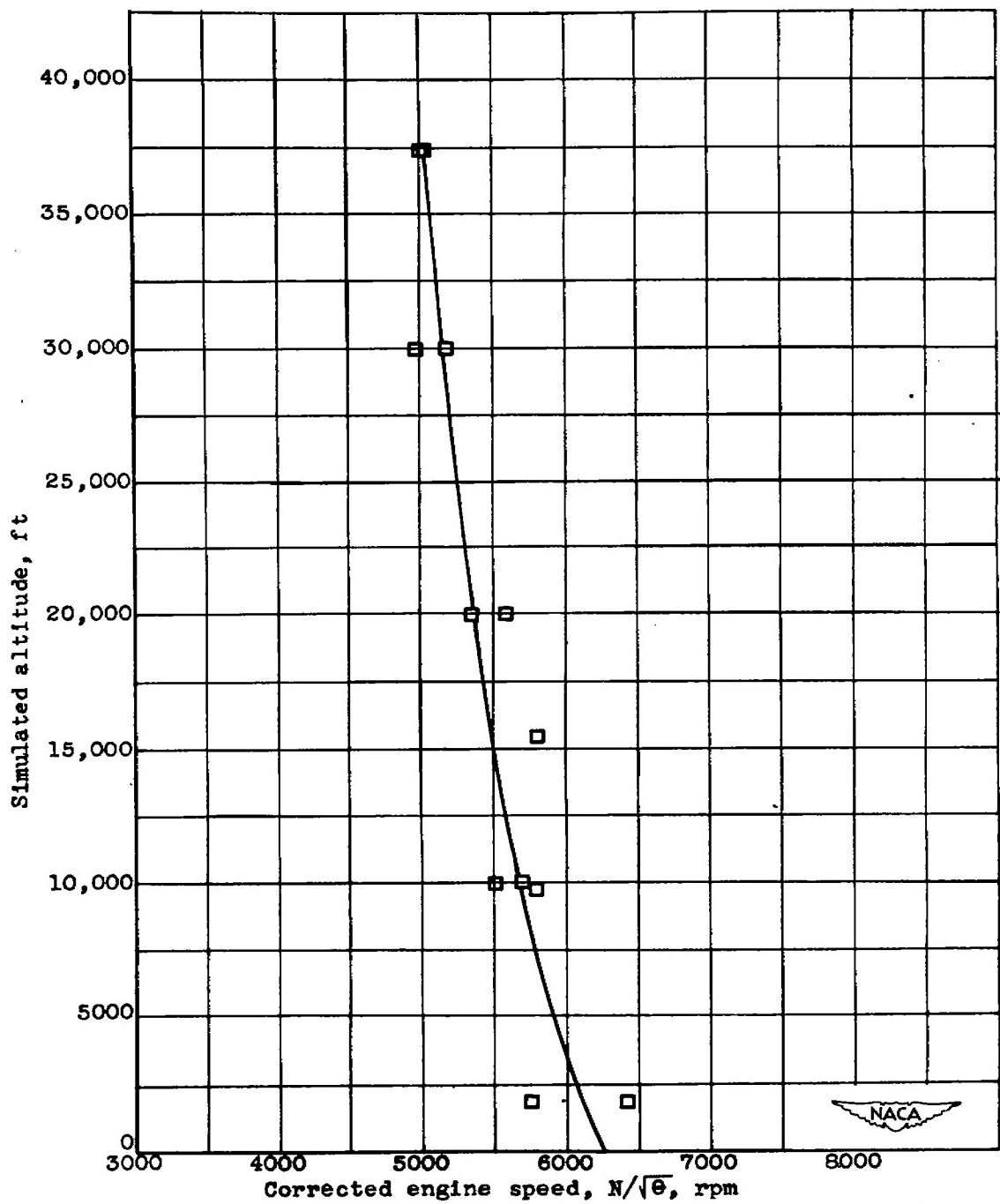
Figure 28.— Effect of altitude on corrected engine speed
at which compressor stall occurred at static-test con-
ditions. High-flow compressor; small turbine nozzles.